

APPENDIX - FOR ONLINE PUBLICATION

Why Does the Fed Move Markets so Much?
A Model of Monetary Policy and Time-Varying Risk Aversion

Carolin Pflueger and Gianluca Rinaldi¹

June 2022

¹Pflueger: University of Chicago, Harris School of Public Policy, NBER, and CEPR. Email cpflueger@uchicago.edu.
Rinaldi: Harvard University. Email rinaldi@g.harvard.edu.

A. Model Appendix

A.1. Loglinear habit dynamics around steady state

We derive a loglinear expansion showing that we can view habit approximately as a function of current and lagged consumption moments. This Section derives the loglinear dynamics of the habit stock using a first order approximation around the steady state $S_t = \bar{S}$. We write log habit h_t as a distributed lag of current and lagged consumption moments and the output gap, which also equals stochastically de-trended consumption according to model equation (10).

We model how habit adjusts to consumption implicitly by modeling the evolution of the log surplus consumption ratio. In order to solve for log habit we need an approximate relation between log habit, log consumption, and the log surplus consumption ratio. Defining $\hat{s}_t = s_t - \bar{s}$, we develop a first-order Taylor expansion of \hat{s}_t in terms of $c_t - h_t$. We take the first derivative of \hat{s}_t with respect to $c_t - h_t$:

$$\frac{d\hat{s}_t}{d(c_t - h_t)} = \frac{d}{d(c_t - h_t)} \left(\log \left(\frac{1 - \exp(-(c_t - h_t))}{\bar{S}} \right) \right), \quad (\text{A1})$$

$$= \frac{\bar{S}}{1 - \exp(-(c_t - h_t))} \frac{\exp(-(c_t - h_t))}{\bar{S}}, \quad (\text{A2})$$

$$= - \left(1 - \frac{1}{S_t} \right), \quad (\text{A3})$$

so at the steady state this first derivative equals:

$$\left. \frac{d\hat{s}_t}{d(c_t - h_t)} \right|_{S_t = \bar{S}} = - \left(1 - \frac{1}{\bar{S}} \right). \quad (\text{A4})$$

The first order Taylor expansion for \hat{s}_t in terms of $c_t - h_t$ around the steady-state therefore equals (up to constant):

$$\hat{s}_t \approx \left(1 - \frac{1}{\bar{S}} \right) (h_t - c_t), \quad (\text{A5})$$

or

$$h_t \approx c_t + \frac{\hat{s}_t}{1 - \frac{1}{\bar{S}}}. \quad (\text{A6})$$

The relation (A6) is approximate rather than exact because we ignore second- and higher-order terms in $(c_t - h_t)$. Further approximating $\lambda(s_t) \approx \lambda(\bar{s}) = \frac{1}{\bar{S}} - 1$, the approximate dynamics for \hat{s}_t near the steady state are given by:

$$\hat{s}_{t+1} \approx \theta_0 \hat{s}_t + \theta_1 x_t + \theta_2 x_{t-1} + \left(\frac{1}{\bar{S}} - 1 \right) \varepsilon_{c,t+1}. \quad (\text{A7})$$

Combining (A6) with (A7) gives the approximate dynamics for log habit:

$$h_{t+1} \approx c_{t+1} + \frac{1}{1 - \frac{1}{\bar{S}}} \hat{s}_{t+1}, \quad (\text{A8})$$

$$\approx c_{t+1} + \frac{1}{1 - \frac{1}{\bar{S}}} \left(\theta_0 \hat{s}_t + \theta_1 x_t + \theta_2 x_{t-1} + \varepsilon_{s,t} + \left(\frac{1}{\bar{S}} - 1 \right) \varepsilon_{c,t+1} \right), \quad (\text{A9})$$

$$\approx c_{t+1} - \varepsilon_{c,t+1} + \theta_0 (h_t - c_t) - \frac{\theta_1}{\frac{1}{\bar{S}} - 1} x_t - \frac{\theta_2}{\frac{1}{\bar{S}} - 1} x_{t-1}, \quad (\text{A10})$$

$$\approx \theta_0 h_t + (1 - \theta_0) c_t + E_t \Delta c_{t+1} - \frac{\theta_1 x_t + \theta_2 x_{t-1}}{\frac{1}{\bar{S}} - 1}, \quad (\text{A11})$$

where we use $\Delta c_{t+1} = c_{t+1} - c_t$ to denote the change in log consumption from time t to time $t + 1$. We

now iterate (A11) to obtain:

$$h_{t+1} \approx \sum_{j=0}^{\infty} \theta_0^j \left((1 - \theta_0)c_{t-j} + E_{t-j}\Delta c_{t-j+1} - \frac{\theta_1 x_{t-j} + \theta_2 x_{t-j-1}}{\frac{1}{\bar{s}} - 1} \right), \quad (\text{A12})$$

$$\approx (1 - \theta_0) \sum_{j=0}^{\infty} \theta_0^j c_{t-j} + \sum_{j=0}^{\infty} \theta_0^j E_{t-j}\Delta c_{t-j+1} - \frac{\theta_1}{\frac{1}{\bar{s}} - 1} x_t \quad (\text{A13})$$

$$- \frac{\theta_0 \theta_1 + \theta_2}{\frac{1}{\bar{s}} - 1} \sum_{j=0}^{\infty} \theta_0^j x_{t-j-1}. \quad (\text{A14})$$

The expansion (A14) shows that approximate log habit depends on lagged moments of consumption and the output gap.

We substitute in for the output gap x_t from equation (10) in the main paper:

$$h_{t+1} \approx (1 - \theta_0) \sum_{j=0}^{\infty} \theta_0^j c_{t-j} + \sum_{j=0}^{\infty} \theta_0^j E_{t-j}\Delta c_{t-j+1} \quad (\text{A15})$$

$$- \frac{\theta_1}{\frac{1}{\bar{s}} - 1} \left(c_t - (1 - \phi) \sum_{i=0}^{\infty} \phi^i c_{t-1-i} \right) \quad (\text{A16})$$

$$- \frac{\theta_0 \theta_1 + \theta_2}{\frac{1}{\bar{s}} - 1} \sum_{j=0}^{\infty} \theta_0^j \left(c_{t-j-1} - (1 - \phi) \sum_{i=0}^{\infty} \phi^i c_{t-j-2-i} \right). \quad (\text{A17})$$

The [Campbell and Cochrane \(1999\)](#) case corresponds to $\theta_1 = \theta_2 = 0$ and constant expected consumption growth. In that case, expression (A17) shows that log habit is approximately an exponentially-weighted moving average of lagged log consumption with exponential parameter θ_0 .

In our calibration $\theta_1 < 0$ and $\theta_2 > 0$ and we impose the constraint that the lead and lag coefficients in the New Keynesian Euler equation sum up to one, i.e. equation (16) in the main paper. With this additional constraint, the loading of log habit onto the first two lags of consumption at the steady-state become

$$\frac{\partial h_{t+1}}{\partial c_t} = (1 - \theta_0) - \frac{\theta_1}{\frac{1}{\bar{s}} - 1}, \quad (\text{A18})$$

$$\frac{\partial h_{t+1}}{\partial c_{t-1}} = (1 - \theta_0)\theta_0 + \frac{\theta_1(1 - \phi) - \theta_0\theta_1 - \theta_2}{\frac{1}{\bar{s}} - 1}, \quad (\text{A19})$$

$$= (1 - \theta_0)\theta_0 + \frac{1 - \phi}{\frac{1}{\bar{s}} - 1} + ((1 - \phi) + (1 - \theta_0)) \times \frac{\theta_1}{\frac{1}{\bar{s}} - 1}. \quad (\text{A20})$$

Equation (A18) shows that a negative value for θ_1 (as in our calibration) drives up habit's loading on the most recent consumption lag. Because ϕ and θ_0 are both close to but smaller than one, equation (A20) shows that $\frac{\partial h_{t+1}}{\partial c_{t-1}}$ also increases when θ_1 is negative. However, $\frac{\partial h_{t+1}}{\partial c_{t-1}}$ changes much less with θ_1 than $\frac{\partial h_{t+1}}{\partial c_t}$ because in (A20) θ_1 is pre-multiplied by a small factor $((1 - \phi) + (1 - \theta_0))$. In our calibration $((1 - \phi) + (1 - \theta_0)) = 0.10$, so a negative value for θ_1 increases habit's dependence on the most recent consumption lag, but roughly leaves its dependence on the second consumption lag unchanged.

B. New Keynesian Microfoundations

For completeness, in this Section we present a set of microfoundations for the log-linearized macroeconomic New Keynesian model with finance habit formation preferences. We make some minor modifications to the standard setup and derivation to address the issues noted by Lettau and Uhlig (2000) that habit may affect labor supply decisions in a production economy, and to ensure that model output gap is level stationary whereas consumption is stationary in changes, i.e. equation (10) in the main paper.

B.1. Firms

B.1.1. Final good

A final consumption good Y_t is produced by a representative perfectly competitive firm from a continuum of differentiated goods $Y_{i,t}$:

$$Y_t \equiv \left[\int_0^1 Y_{i,t}^{\frac{\zeta-1}{\zeta}} di \right]^{\frac{\zeta}{\zeta-1}}. \quad (\text{A21})$$

The resulting demand for the differentiated good i is downward-sloping in its product price $P_{i,t}$:

$$Y_{i,t} = Y_t \left(\frac{P_{i,t}}{P_t} \right)^{-\zeta}. \quad (\text{A22})$$

Here, $P_t = \left[\int_0^1 P_{i,t}^{-(\zeta-1)} di \right]^{-\frac{1}{\zeta-1}}$ is the aggregate price level. The constant ζ is the elasticity of substitution across intermediate goods.

B.1.2. Intermediate good

Intermediate goods firm i produces according to a Cobb-Douglas production function with capital share τ :

$$Y_{i,t} = N_t L_{i,t}^{1-\tau}. \quad (\text{A23})$$

Productivity is given by N_t . With (A21), aggregate output then satisfies

$$Y_t = N_t L_t^{1-\tau}, \quad (\text{A24})$$

where aggregate labor is defined:

$$L_t \equiv \left[\int_0^1 L_{i,t}^{\frac{(\zeta-1)(1-\tau)}{\zeta}} di \right]^{\frac{\zeta}{(\zeta-1)(1-\tau)}}. \quad (\text{A25})$$

The aggregate resource constraint in this economy is simple. Because there is no time-varying real investment, consumption equals output $C_t = Y_t$.

Following Lucas (1988), we assume that human capital depends on the average skill acquired by all agents, and that changes in log human capital are driven by past market labor, l_{t-1} :

$$n_t = \nu + n_{t-1} + (1 - \phi)(1 - \tau)l_{t-1}. \quad (\text{A26})$$

Here, $0 \leq \phi \leq 1$ and $\nu > 0$ are constants. This assumption ensures that potential output increases with lagged output. The process (A26) can equivalently be interpreted as a simple endogenous capital stock, similarly to (Woodford, 2003, Chapter 5), if a fixed proportion of market labor each period is used to produce investment goods and we scale the total amount of labor available accordingly.

Intermediate firm profit equals output minus the cost of labor, subject to the production function (A23), demand for differentiated goods (A22), and taking wages as given.

B.1.3. Price setting

Intermediate firms face standard price-setting frictions in the manner of Calvo (1983), where fraction $1 - \alpha$ of firms can change prices every period with equal probabilities across firms. When firms cannot update, their prices are indexed to lagged inflation (Smets and Wouters (2007), Christiano, Eichenbaum, and Evans (2005)). A firm that last reset its price at time t to \tilde{P}_t , charges a nominal time $t + j$ price $\tilde{P}_t \left(\frac{P_{t-1+j}}{P_{t-1}} \right)$. A firm that can update its product price maximizes the discounted sum of current and future expected profits while the price is expected to remain in place, discounted at the households' stochastic discount factor.

B.2. Labor-leisure choice

The wages intermediate firms face arise from a standard labor-leisure choice. The habit preferences over market consumption in Section 2.1 in the main paper arise when leisure and home good habits are at their equilibrium values.

Following the classic model of Greenwood, Hercowitz, and Huffman (1988), we assume that total consumption consists of market consumption and home produced goods. Labor not used in the market is used for home production, such as cooking at home instead of eating out. Household H 's total consumption is the sum of market consumption, $C_{h,t}$, and home production $C_{h,t}^{home}$:

$$C_{h,t}^{home} = N_t \frac{\int_0^1 (1 - L_{h,i,t})^{1-\chi} di}{1 - \chi}. \quad (\text{A27})$$

Here, $L_{h,i,t}$ denotes the differentiated labor that household h provides to firm i and $(1 - L_{h,i,t})$ is labor used for home production. Home production has decreasing returns to scale, as in Campbell and Ludvigson (2001), and the parameter χ determines the elasticity of market labor supply.² Utility equals

$$U_{h,t} = \frac{\left((C_{h,t} - H_t) + (C_{h,t}^{home} - H_t^{home}) \right)^{1-\gamma} - 1}{1 - \gamma} \quad (\text{A28})$$

Both market and home consumption are assumed to be subject to external habits, H_t and H_t^{home} . Habits are external, meaning that they are shaped by aggregate consumption and labor rather than household h 's own consumption and labor. The parameter γ is a curvature parameter.

The formulation of the labor-leisure choice following Greenwood, Hercowitz, and Huffman (1988) separates the intratemporal labor-leisure choice from the intertemporal consumption-savings decision, which is needed to ensure that the intermediate firms' first-order profit takes a standard form. The assumption that productivity in the home increases with aggregate productivity, N_t , ensures that the labor-leisure trade-off does not become irrelevant over time consistent with empirical evidence (Kehoe, Lopez, Midrigan, Pastorino (2019), Chodorow-Reich and Karabarbounis (2016)). A complementary approach to separate wages from consumption habit would be to introduce separate slow-moving habits for consumption and leisure combined with labor market frictions, though matching asset pricing moments can be challenging in such a setup (Uhlig (2007), Rudebusch (2008), Lopez (2014)). Our formulation is more parsimonious and requires only one parameter, χ , closely related to the Frisch elasticity of labor supply. Because of this parsimony we consider our model a useful template to study the interaction between labor market frictions and habits in future research.

B.2.1. Home and market good habits

As in Campbell and Cochrane (1999) all habits are external. We assume that home good habit equals aggregate home good consumption, i.e. $H_{h,t}^{home} = C_{h,t}^{home}$ for all households h . When home goods consumption is at its equilibrium value $C_{h,t}^{home} = C_t^{home}$, utility over market consumption therefore takes the form (1) in the main paper. Market consumption habit is described by equations (4) through (9) in the main paper.

B.3. Overview: Proof of Phillips Curve

We now derive the log-linearized Phillips curve (23) from the firm's optimal price-setting and production problems. This derivation is tedious, but almost all the steps in our derivation are standard. Our asset pricing habit preferences potentially enter in two places. This Section shows that the log-linearized Phillips curve is invariant to both of these channels for the following two reasons:

1. Firms' real marginal cost depends on the real wage, which depends on preferences. The log-linearized Phillips curve is invariant to this channel, because we separate the intertemporal

²The differentiated labor assumption follows Woodford (2003, Chapter 3) and generates real rigidities from labor immobility across sectors (Ball and Romer (1990)).

consumption-savings decision and the intratemporal labor-leisure choice as in Greenwood, Hercowitz, and Huffman (1988). We therefore obtain a standard functional form for log-linearized real marginal cost that does not depend on habit or surplus consumption.

2. The SDF enters into firms' first-order condition for the optimal price-setting decision. The log-linearized Phillips curve is invariant to this channel, because up to first-order our SDF is standard and second-order terms drop out of the log-linearized first-order condition, leading to a standard log-linearized Phillips curve.

We log linearize labor around the steady-state with $\bar{Y}_t = \bar{L}^{1-\tau}$ and \bar{L} the labor supply consistent with steady-state markups when prices are flexible. We use bars to denote steady-state values and hats to denote log deviations from this steady-state. We use lower-case letters to denote logs.

B.4. Marginal cost of production and steady-state labor supply

In this Section, we follow standard log-linearization steps to show that to first order firm i ' log deviation of marginal cost from steady-state takes the form:

$$\hat{m}c_{i,t} = a_0 \hat{y}_t - a_1 (p_{i,t} - p_t), \quad (\text{A29})$$

i.e. it increases in the log deviation of output from the steady state, and decreases in the log own-firm price deviation from the log aggregate price level where both a_0 and a_1 are positive constants. We use hats to denote log deviations from the steady-state, so that $\hat{y}_t = x_t$ is the log output gap.

The real wage must equate household h 's marginal disutility of labor outside the home with the marginal utility of market consumption:

$$W_{i,t} = \frac{\frac{\partial U_{h,t}}{\partial L_{h,i,t}}}{\frac{\partial U_{h,t}}{\partial C_{h,t}}} = N_t (1 - L_{h,i,t})^{-\chi}. \quad (\text{A30})$$

Because all households are identical, this means that the wage for labor of type i must equal

$$W_{i,t} = N_t (1 - L_{i,t})^{-\chi}. \quad (\text{A31})$$

Firm i 's cost of producing quantity $Y_{i,t}$ of good i equals:

$$\text{Cost}_{i,t} = W_{i,t} L_{i,t} \quad (\text{A32})$$

$$= W_{i,t} \left(\frac{Y_{i,t}}{N_t} \right)^{1/(1-\tau)} \quad (\text{A33})$$

Taking the derivative with respect to $Y_{i,t}$ and substituting in for the wage from (A31) gives the marginal cost of supplying good i :

$$MC_{i,t} = \frac{1}{1-\tau} \frac{W_{i,t}}{N_t} \left(\frac{Y_{i,t}}{N_t} \right)^{\frac{\tau}{1-\tau}}, \quad (\text{A34})$$

$$= \frac{1}{1-\tau} \left(1 - \left(\frac{Y_{i,t}}{N_t} \right)^{1/(1-\tau)} \right)^{-\chi} \left(\frac{Y_{i,t}}{N_t} \right)^{\frac{\tau}{1-\tau}}. \quad (\text{A35})$$

Note that here we have assumed that the producer is a wage taker following Woodford (2003, p.148). We define the steady-state labor supply \bar{L} to be the amount of labor supplied if markups are equal to the steady-state value

$$\mu \equiv \frac{\zeta}{1-\zeta} \quad (\text{A36})$$

, and all firms charge the same price. From (A35), the steady-state labor supply \bar{L} then is the unique

solution to

$$\mu^{-1} = \frac{1}{1-\tau} (1-\bar{L})^{-\chi} \bar{L}^{\frac{\tau}{1-\tau}}. \quad (\text{A37})$$

At the steady-state the real wage for labor of type i equals

$$\bar{W}_{i,t} = N_t (1-\bar{L})^{-\chi}. \quad (\text{A38})$$

Log-linearizing the real wage around the steady-state wage gives:

$$\hat{w}_{i,t} = \chi \frac{\bar{L}}{1-\bar{L}} \hat{l}_{i,t}, \quad (\text{A39})$$

$$= \eta \hat{l}_{i,t}. \quad (\text{A40})$$

Here,

$$\eta \equiv \chi \frac{\bar{L}}{1-\bar{L}} \quad (\text{A41})$$

is the inverse of the steady-state Frisch elasticity of labor supply.

Intermediate firm i 's elasticity of real marginal cost with respect to own-firm output near the steady-state then equals:

$$\frac{dMC_{i,t}}{dY_{i,t}} \frac{Y_{i,t}}{MC_{i,t}} = \frac{\tau}{1-\tau} + \frac{\eta}{1-\tau}, \quad (\text{A42})$$

$$\equiv \omega. \quad (\text{A43})$$

To first order, firm i 's log marginal cost relative to steady-state then equals

$$\begin{aligned} \widehat{mc}_{i,t} &= \log(MC_{i,t}) - \log(\mu^{-1}), \\ &= \omega \hat{y}_{i,t}, \end{aligned} \quad (\text{A44})$$

$$= \omega \hat{y}_t - \omega \zeta (p_{i,t} - p_t), \quad (\text{A45})$$

In the last step, we have used the demand function (A22). We hence obtain the functional form (A29) with $a_0 = \omega$ and $a_1 = \omega \zeta$.

We can compare (A45) to the log real marginal cost obtained with standard preferences (e.g. Woodford, 2003), where the real wage is given by

$$W_t = \frac{L_{i,t}^\eta}{C_t^{1-\gamma}}, \quad (\text{A46})$$

where η is the inverse of the Frisch elasticity of labor supply and γ is risk aversion. This expression is log-linearized to

$$\hat{w}_{i,t} = \gamma \hat{y}_t + \eta \hat{l}_{i,t}. \quad (\text{A47})$$

If instead, the log-linearized real wage took the form (A47), we would obtain the following log-linearized expression for the real marginal cost:

$$\widehat{mc}_{i,t} = (\omega + \gamma) \hat{y}_t - \omega \zeta (p_{i,t} - p_t), \quad (\text{A48})$$

i.e. $a_0 = \omega + \gamma$ and $a_1 = \omega \zeta$. Comparing expressions (A45) and (A48) shows that the log-linearized real wage in our model takes the same functional form as under standard preferences.

B.5. Discount Factor for Phillips Curve

We now derive the first-order approximation of the stochastic discount factor. Let $M_{t,t+j} = M_{t+1}M_{t+2}\dots M_{t+j}$ denote the household SDF for discounting cash flows at time $t+j$ back to time t . In the steady-state, log consumption grows at rate g and s_t is constant at \bar{s} . The steady-state SDF for discounting time $t+j$ real cash flows at time t takes the standard form:

$$\bar{M}_{t,t+j} = \beta^j \exp(-\gamma g j). \quad (\text{A49})$$

We denote log deviation of the SDF from this steady-state:

$$\hat{m}_{t,t+j} = \log(M_{t,t+j}/\bar{M}_{t,t+j}). \quad (\text{A50})$$

We will see that $\hat{m}_{t,t+j}$ drops out of the log-linearized price-setting first-order condition.

B.6. Price Level Law of Motion

The remainder of the derivation of the log-linearized profit first-order condition is standard and follows Walsh (2017). We log-linearize around $\pi_t = 0$.

Since the probability of being able to adjust the price-level is independent and equal across firms, each firm that has the chance to re-set its price at time t chooses the same price \tilde{P}_t . The law of motion for the price level is

$$P_t^{-(\zeta-1)} = \alpha \left(P_{t-1} \frac{P_{t-1}}{P_{t-2}} \right)^{-(\zeta-1)} + (1-\alpha) \tilde{P}_t^{-(\zeta-1)}. \quad (\text{A51})$$

Dividing (A51) by $P_t^{-(\zeta-1)}$ gives

$$1 = \alpha \exp((\zeta-1)(\pi_t - \pi_{t-1})) + (1-\alpha) \left(\frac{\tilde{P}_t}{P_t} \right)^{-(\zeta-1)}. \quad (\text{A52})$$

Using the notation $\tilde{p}_t = \log\left(\frac{\tilde{P}_t}{P_t}\right)$, to first-order the price-level law of motion is

$$\tilde{p}_t = \frac{\alpha}{1-\alpha} (\pi_t - \pi_{t-1}). \quad (\text{A53})$$

B.7. Price-Setting First-Order Condition

The price charged at time $t+j$ by a firm that last got to reset its price at time t equals

$$\tilde{P}_t (P_{t-1+j}/P_{t-1}). \quad (\text{A54})$$

A firm that has the opportunity to re-set prices at time t chooses the price \tilde{P}_t to maximize the expected discounted sum of real profits conditional on the price still being in place:

$$\max_{\tilde{P}_t} E_t^e \sum_{j=0}^{\infty} \alpha^j M_{t,t+j} Y_{t+j} \left(\left(\frac{\tilde{P}_t P_{t-1+j}/P_{t-1}}{P_{t+j}/P_t} \right)^{1-\zeta} - \frac{Cost_{t,t+j}}{Y_{t+j}} \right), \quad (\text{A55})$$

where we use superscript e to denote price-setters' expectations.

The first-order condition with respect to the optimal price \tilde{P}_t equates the expected discounted sum of the marginal change in revenue with the expected discounted sum of the marginal change in cost of

producing the quantity demanded

$$\begin{aligned} & \frac{\tilde{P}_t}{P_t} E_t^e \sum_{j=0}^{\infty} \alpha^j M_{t,t+j} Y_{t+j} (\zeta - 1) \left(\frac{P_{t-1+j}/P_{t-1}}{P_{t+j}/P_t} \right)^{1-\zeta} \\ &= E_t^e \sum_{j=0}^{\infty} \alpha^j M_{t,t+j} Y_{t+j} \zeta \left(\frac{P_{t-1+j}/P_{t-1}}{P_{t+j}/P_t} \right)^{-\zeta} MC_{i,t+j}. \end{aligned} \quad (\text{A56})$$

B.8. Log-Linearizing the Profit First-Order Condition

We now log-linearize the first-order condition (A56) following the steps outlined in Walsh (2017), Chapter 8.7. In the flexible-price equilibrium, all firms charge the same price so $\overline{MC} = \mu^{-1} = \frac{\zeta-1}{\zeta}$. Denoting the log of steady-state output by $\bar{y}_t \equiv \log \bar{Y}_t$ we have that

$$\bar{y}_{t+1} - \bar{y}_t = \Delta n_{t+1}, \quad (\text{A57})$$

$$= \nu + (1 - \phi)(1 - \tau)l_t, \quad (\text{A58})$$

$$= g + (1 - \phi)\hat{y}_t, \quad (\text{A59})$$

where the steady-state growth rate, g , equals

$$g = \nu + (1 - \phi)(1 - \tau)\bar{l}. \quad (\text{A60})$$

To save on notation, we define:

$$\beta_g = \beta \exp(-(\gamma - 1)g). \quad (\text{A61})$$

The log-linear expansion for the left-hand-side of (A56) conditional on \bar{Y}_t becomes:

$$\begin{aligned} & (1 + \tilde{p}_t) E_t^e \sum_{j=0}^{\infty} \left[(\beta_g \alpha)^j \bar{Y}_t (1 + \hat{y}_{t+j}) (1 + (\bar{y}_{t+j} - \bar{y}_t - g)) (1 + \hat{m}_{t,t+j}) (\zeta - 1) \times \right. \\ & \left. (1 + (1 - \zeta)(\pi_t - \pi_{t+j})) \right]. \end{aligned} \quad (\text{A62})$$

Dropping second-order terms and collecting terms that are independent of horizon j gives

$$\begin{aligned} & \frac{\bar{Y}_t(\zeta - 1)}{1 - \beta_g \alpha} + \frac{\bar{Y}_t \tilde{p}_t (\zeta - 1)}{1 - \beta_g \alpha} \\ & + \bar{Y}_t (\zeta - 1) E_t^e \sum_{j=0}^{\infty} (\beta_g \alpha)^j (\hat{y}_{t+j} + (\bar{y}_{t+j} - \bar{y}_t - g) + \hat{m}_{t,t+j} + (1 - \zeta)(\pi_t - \pi_{t+j})). \end{aligned} \quad (\text{A63})$$

Next, we approximate the right-hand-side of (A56) log-linearly. This gives

$$\begin{aligned} & E_t^e \sum_{j=0}^{\infty} \left[(\beta_g \alpha)^j \bar{Y}_t (1 + \hat{y}_{t+j}) (1 + (\bar{y}_{t+j} - \bar{y}_t - g)) (1 + \hat{m}_{t,t+j}) \zeta \times \right. \\ & \left. (1 - \zeta(\pi_t - \pi_{t+j})) \overline{MC} (1 + \widehat{m}_{t,t+j}) \right]. \end{aligned} \quad (\text{A64})$$

Next, we use $\zeta \overline{MC} = \zeta - 1$, substitute in (A45), and drop second-order terms:

$$\begin{aligned} & \frac{\bar{Y}_t(\zeta - 1)}{1 - \beta_g \alpha} + \bar{Y}_t(\zeta - 1) E_t^e \sum_{j=0}^{\infty} (\beta_g \alpha)^j (\hat{y}_{t+j} + (\bar{y}_{t+j} - \bar{y}_t - g) + \hat{m}_{t,t+j}) \\ & + \bar{Y}_t(\zeta - 1) E_t^e \sum_{j=0}^{\infty} (\beta_g \alpha)^j (-\zeta (\pi_t - \pi_{t+j}) + \widehat{mc}_{t+j}), \end{aligned} \quad (\text{A65})$$

$$\begin{aligned} = & \frac{\bar{Y}_t(\zeta - 1)}{1 - \beta_g \alpha} + \bar{Y}_t(\zeta - 1) E_t^e \sum_{j=0}^{\infty} (\beta_g \alpha)^j (\hat{y}_{t+j} + (\bar{y}_{t+j} - \bar{y}_t - g) + \hat{m}_{t,t+j}) \\ & + \bar{Y}_t(\zeta - 1) E_t^e \sum_{j=0}^{\infty} (\beta_g \alpha)^j (-\zeta (\pi_t - \pi_{t+j}) + a_0 \hat{y}_{t+j}) \\ & - a_1 \left(\frac{\bar{Y}_t(\zeta - 1) \tilde{p}_t}{1 - \beta_g \alpha} + \bar{Y}_t(\zeta - 1) E_t^e \sum_{j=0}^{\infty} (\beta_g \alpha)^j (\pi_t - \pi_{t+j}) \right). \end{aligned} \quad (\text{A66})$$

Equating (A63) and (A66), cancelling common terms, and dividing by $\bar{Y}_t(\zeta - 1)$ gives

$$\begin{aligned} & (1 + a_1) \left(\frac{\tilde{p}_t}{1 - \beta_g \alpha} + \frac{\pi_t}{1 - \beta_g \alpha} - E_t^e \sum_{j=0}^{\infty} (\beta_g \alpha)^j \pi_{t+j} \right) \\ & = E_t \sum_{j=0}^{\infty} (\beta_g \alpha)^j (a_0 \hat{y}_{t+j}). \end{aligned} \quad (\text{A67})$$

Note in particular that $\hat{m}_{t,t+j}$ drops out of (A67). Because this is the main place where we differ from the standard New Keynesian model, this makes clear that our asset pricing preferences drop out of the log-linearized optimal price-setting decision.

B.9. Substituting out \tilde{p}_t

Next, we follow a number of standard steps (e.g. Walsh (2017)) to solve for π_t . From equation (A67) we have:

$$\begin{aligned} \tilde{p}_t + \pi_t &= (1 - \beta_g \alpha) E_t^e \sum_{j=0}^{\infty} (\beta_g \alpha)^j \left(\frac{a_0 \hat{y}_{t+j}}{1 + a_1} + \pi_{t+j} \right), \quad (\text{A68}) \\ &= \frac{1 - \beta_g \alpha}{1 + a_1} (a_0 \hat{y}_t) + (1 - \beta_g \alpha) \pi_t \\ &\quad + \beta_g \alpha (1 - \beta_g \alpha) E_t^e \sum_{j=0}^{\infty} (\beta_g \alpha)^j \left(\frac{a_0 \hat{y}_{t+1+j}}{1 + a_1} + \pi_{t+1+j} \right), \\ &= \frac{1 - \beta_g \alpha}{1 + a_1} (a_0 \hat{y}_t) + (1 - \beta_g \alpha) \pi_t + \beta_g \alpha E_t^e (\tilde{p}_{t+1} + \pi_{t+1}) \end{aligned} \quad (\text{A69})$$

This equation relates the optimal relative price to the current-period marginal cost, current-period optimal markup, and the next-period expected optimal relative price. Subtracting π_t from both sides gives

$$\tilde{p}_t = \frac{1 - \beta_g \alpha}{1 + a_1} (a_0 \hat{y}_t) - \beta_g \alpha \pi_t + \beta_g \alpha E_t^e \pi_{t+1} + \beta_g \alpha E_t^e \tilde{p}_{t+1}. \quad (\text{A70})$$

Substituting in the log-linearized law of motion for inflation (A53) and multiplying by $\frac{1-\alpha}{\alpha}$ gives

$$(\pi_t - \pi_{t-1}) = \frac{1 - \alpha}{\alpha} \frac{1 - \beta_g \alpha}{1 + a_1} (a_0 \hat{y}_t) - \beta_g \pi_t + \beta_g E_t^e \pi_{t+1} \quad (\text{A71})$$

Solving for π_t gives the New Keynesian Phillips Curve (ignoring constants)

$$\pi_t = \frac{\beta_g}{1 + \beta_g} \pi_t^e + \frac{1}{1 + \beta_g} \pi_{t-1} + \kappa \hat{y}_t, \quad (\text{A72})$$

where π_t^e denotes price-setters's inflation expectations and the Phillips curve slope coefficient on $\hat{y}_t = x_t$ equals

$$\kappa = \frac{1}{1 + \beta_g} \frac{1 - \alpha}{\alpha} (1 - \beta_g \alpha) \frac{a_0}{1 + a_1}. \quad (\text{A73})$$

Finally, we use that (up to a constant)

$$x_t = \hat{y}_t, \quad (\text{A74})$$

$$a_0 = \omega, \quad (\text{A75})$$

$$a_1 = \omega \zeta. \quad (\text{A76})$$

to obtain the log-linearized New Keynesian Phillips curve (23) in the main paper. One way to obtain a backward-looking coefficient in the Phillips curve that is not as closely tied to β_t and that can therefore be matched more closely to the empirical persistence of inflation is if price-setters' inflation expectations are partially indexed to lagged inflation ($\pi_t^e = \rho^e \pi_{t-1} + (1 - \rho^e) E_t \pi_{t+1}$, for some constant $\rho^e \in [0, 1]$ where $E_t \pi_{t+1}$ is the rational forecast of next-period inflation). In that case the backward-looking component in the Phillips curve equals $\rho^\pi = \frac{1}{1 + \beta_g} + \frac{\beta_g}{1 + \beta_g} r h o^e$. Other ways to obtain a larger backward-looking component in the Phillips curve would be through more complicated price-setting mechanisms (e.g. Fuhrer and Moore (1995)).

Note that the limiting case of perfectly sticky prices ($\alpha = 0$) corresponds to $\kappa = 0$, so inflation equals zero irrespective of the cross-goods substitutability ζ . The parameters τ and η also drop out of equilibrium dynamics in that case, simplifying the macroeconomic dynamics.

C. Model Solution

C.1. Consumption from output gap

Recall that the steady-state is given by $\bar{Y}_t = N_t \bar{L}^{1-\tau}$, where \bar{L} is the labor supply consistent with flexible prices and steady-state markups.

Using the resource constraint $y_t = c_t$ and the process for human capital (A26).

$$n_t = \nu + n_{t-1} + (1 - \phi)(1 - \tau)l_{t-1}, \quad (\text{A77})$$

$$= \nu + n_{t-1} + (1 - \phi)y_{t-1}, \quad (\text{A78})$$

$$= \frac{\nu}{1 - \phi} + (1 - \phi) \sum_{j=0}^{\infty} \phi^j y_{t-1-j}. \quad (\text{A79})$$

The deviation of output from the flexible-price equilibrium then equals (up to a constant):

$$x_t = y_t - n_t, \quad (\text{A80})$$

$$= y_t - (1 - \phi) \sum_{j=0}^{\infty} \phi^j (y_{t-1-j}), \quad (\text{A81})$$

$$= c_t - (1 - \phi) \sum_{j=0}^{\infty} \phi^j c_{t-1-j}, \quad (\text{A82})$$

i.e. equation (10) in the main paper. Inverting equation (10) gives the equilibrium consumption dynamics

from the output gap:

$$\Delta c_{t+1} = x_{t+1} - \phi x_t. \quad (\text{A83})$$

We can therefore solve for consumption from the output gap and vice versa.

C.2. Details: Euler equation derivation

With the updating equation for log consumption growth (A83), the asset pricing Euler equation for the one-period real risk-free rate is given by:

$$r_t = \gamma E_t \Delta c_{t+1} + \gamma E_t \Delta \hat{s}_{t+1} - \frac{\gamma^2}{2} (1 + \lambda(s_t))^2 \sigma_c^2, \quad (\text{A84})$$

$$= \gamma E_t \Delta c_{t+1} + \gamma(\theta_0 - 1)\hat{s}_t + \gamma\theta_1 x_t + \gamma\theta_2 x_{t-1} - \frac{\gamma^2}{2} (1 + \lambda(s_t))^2 \sigma_c^2, \quad (\text{A85})$$

$$= \gamma E_t x_{t+1} - \gamma\phi x_t + \gamma(\theta_0 - 1)\hat{s}_t + \gamma\theta_1 x_t + \gamma\theta_2 x_{t-1} - \frac{\gamma^2}{2} (1 + \lambda(s_t))^2 \sigma_c^2$$

The sensitivity function has just the right form so that surplus consumption \hat{s}_t drops out and (up to a constant):

$$r_t = \gamma E_t x_{t+1} - \gamma\phi x_t + \gamma\theta_1 x_t + \gamma\theta_2 x_{t-1} \quad (\text{A86})$$

Rearranging and continuing to ignore constants gives:

$$x_t = \frac{1}{\phi - \theta_1} E_t x_{t+1} + \frac{\theta_2}{\phi - \theta_1} x_{t-1} - \frac{1}{\gamma(\phi - \theta_1)} r_t. \quad (\text{A87})$$

Note that we have not made any approximations in the derivation of (14).

C.3. Solving for macroeconomic dynamics

In our solution for macroeconomic dynamics we have several no-longer needed shocks for legacy reasons. The additional shocks - demand, supply, and the shock to the random walk component of inflation - are later set to zero. Our solution method also includes an inflation state variable and a random walk component in inflation, though both are later set to zero.

The full macroeconomic dynamics are given by

$$x_t = f^x E_t x_{t+1} + \rho^x x_{t-1} - \psi (r_t - \gamma \varepsilon_{s,t}), \quad (\text{A88})$$

$$\pi_t = f^\pi E_t \pi_{t+1} + \rho^\pi \pi_{t-1} + \kappa x_t + v_{\pi,t}, \quad (\text{A89})$$

$$i^* = \gamma^x x_t + \gamma^\pi \pi_t + (1 - \gamma^\pi) v_t^*, \quad (\text{A90})$$

$$\hat{i}_t = \rho^i \hat{i}_{t-1} + (1 - \rho^i) i_t^* + v_{MP,t}, \quad (\text{A91})$$

$$v_t^* = v_{t-1}^* + v_{LT,t} \quad (\text{A92})$$

The demand shock $v_{x,t} = \gamma \psi \varepsilon_{s,t}$, the supply shock $v_{\pi,t}$, and the random walk shock $v_{LT,t}$ will later be set to zero, so v_t^* and π_t will also be zero.

We want to find a solution of the form

$$Y_t = B Y_{t-1} + \Sigma v_t, \quad (\text{A93})$$

where the matrix B is $[3 \times 3]$, the matrix Σ is $[3 \times 4]$, and we work with the expanded state vector

$$Y_t = [x_t, \hat{\pi}_t, \hat{i}_t]' \quad (\text{A94})$$

$$, \hat{\pi}_t = \pi_t - v_t^*, \quad (\text{A95})$$

$$\hat{i}_t = i_t - v_t^*. \quad (\text{A96})$$

Writing the macroeconomic dynamics in terms of the state vector Y_t :

$$Y_{1,t} = f^x E_t Y_{1,t+1} + \rho^x Y_{1,t-1} - \psi (Y_{3,t} - E_t Y_{2,t+1}) + v_{x,t}, \quad (\text{A97})$$

$$Y_{2,t} = f^\pi E_t Y_{2,t+1} + \rho^\pi Y_{2,t-1} + \kappa Y_{1,t} + v_{\pi,t} - \rho^\pi v_{LT,t}, \quad (\text{A98})$$

$$Y_{3,t} = \rho^i Y_{3,t-1} + (1 - \rho^i) (\gamma^x Y_{1,t} + \gamma^\pi Y_{2,t}) + v_{ST,t} - \rho^i v_{LT,t}, \quad (\text{A99})$$

$$v_t^* = v_{t-1}^* + v_{LT,t}. \quad (\text{A100})$$

The same thing in matrix form:

$$0 = F E_t Y_{t+1} + G Y_t + H Y_{t-1} + M v_t,$$

where the matrices F , G and H are given by

$$F = \begin{bmatrix} f^x & \psi & 0 \\ 0 & f^\pi & 0 \\ 0 & 0 & 0 \end{bmatrix},$$

$$G = \begin{bmatrix} -1 & 0 & -\psi \\ \kappa & -1 & 0 \\ (1 - \rho^i)\gamma^x & (1 - \rho^i)\gamma^\pi & -1 \end{bmatrix},$$

$$H = \begin{bmatrix} \rho^x & 0 & 0 \\ 0 & \rho^\pi & 0 \\ 0 & 0 & \rho^i \end{bmatrix}.$$

The matrix M is $[3 \times 4]$ and equals:

$$M = \begin{bmatrix} 1 & 0 & 0 & 0 \\ 0 & 1 & 0 & -\rho^\pi \\ 0 & 0 & 1 & -\rho^i \end{bmatrix} \quad (\text{A101})$$

Following Uhlig (1999), we solve for the generalized eigenvectors and eigenvalues of the matrix Ξ with respect to the matrix Δ , where

$$\Xi = \begin{bmatrix} -G & -H \\ I_3 & 0_3 \end{bmatrix}, \quad (\text{A102})$$

$$\Delta = \begin{bmatrix} F & 0_3 \\ 0_3 & I_3 \end{bmatrix} \quad (\text{A103})$$

To obtain a solution, we then pick three generalized eigenvalues $\lambda_1, \lambda_2, \lambda_3$ with generalized eigenvectors $[\lambda z'_1, z'_1]'$, $[\lambda_2 z'_2, z'_2]'$, and $[\lambda_3 z'_3, z'_3]'$. We denote the diagonal matrix of these eigenvalues by $\Lambda = \text{diag}(\lambda_1, \lambda_2, \lambda_3)$, and the matrix of the lower $[3 \times 1]$ portion of the eigenvectors by $\Omega = [z_1, z_2, z_3]$. The corresponding solutions for B and Σ are then given by:

$$B = \Omega \Lambda \Omega^{-1}, \quad (\text{A104})$$

$$\Sigma = -[FB + G]^{-1} M. \quad (\text{A105})$$

In our empirical application, there exist exactly three generalized eigenvalues with absolute value less than one, and we pick the non-explosive solution corresponding to these three eigenvalues.

C.4. Rotated state vector

Our state space for solving for asset prices is five-dimensional: It consists of \tilde{Z}_t , which a scaled version of Y_t , the surplus consumption ratio relative to steady-state \hat{s}_t , and the lagged output gap x_{t-1} . The lagged output gap x_{t-1} is not actually needed as a state variable and we have verified that our numerical solutions for asset prices do not vary with x_{t-1} . Our code includes x_{t-1} as a state variable for legacy reasons.

We next describe the definition of \tilde{Z}_t . To simplify the numerical implementation of the asset pricing recursions, we require that shocks to the scaled state vector \tilde{Z}_t are independent standard normal and that the first dimension of the scaled state vector is perfectly correlated with output gap innovations. This rotation facilitates the numerical analysis, because it is easier to integrate over independent random variables. Aligning the first dimension of the scaled state vector with output gap innovations (and hence surplus consumption innovations) helps, because it allows us to use a finer grid to integrate numerically over this crucial dimension over which asset prices are most non-linear.

If the scaled state vector equals $\tilde{Z}_t = AY_t$ for some invertible matrix A , the dynamics of \tilde{Z}_t are given by:

$$\tilde{Z}_t = AY_t, \quad (\text{A106})$$

$$\tilde{Z}_{t+1} = \underbrace{ABA^{-1}}_{\tilde{B}} \tilde{Z}_t + \underbrace{A\Sigma v_{t+1}}_{\epsilon_{t+1}}. \quad (\text{A107})$$

We hence want a matrix, A , such that

$$\text{Var}(\epsilon_{t+1}) = A\Sigma\Sigma_v\Sigma'A', \quad (\text{A108})$$

$$= \begin{bmatrix} 1 & 0 & 0 \\ 0 & 1 & 0 \\ 0 & 0 & 1 \end{bmatrix}. \quad (\text{A109})$$

Finding such a matrix A should in general be possible, because the matrix M and therefore $\Sigma\Sigma_v\Sigma'$ generally have rank three. We require that the first dimension of ϵ_{t+1} is perfectly correlated with the consumption shock. We can therefore find the three rows of A using the following steps:

1. Set $A_1 = \frac{e_1}{\sqrt{e_1\Sigma\Sigma_v\Sigma'e_1}}$.

2. We use the MATLAB function *null* to compute the null space of $A_1\Sigma\Sigma_v\Sigma'$. Let n_2 denote the first vector in *null* ($A_1\Sigma\Sigma_v\Sigma'$). We then define the second row of A as the normalized version of n_2 :

$$A_2 = \frac{n_2}{\sqrt{n_2\Sigma\Sigma_v\Sigma'n_2'}}$$
(A110)

3. Let n_3 denote the first vector in *null* ($A_1\Sigma\Sigma_v\Sigma', A_2\Sigma\Sigma_v\Sigma'$). We then define the third row of A as the normalized version of n_3 :

$$A_3 = \frac{n_3}{\sqrt{n_3\Sigma\Sigma_v\Sigma'n_3'}}$$
(A111)

It is then straightforward to verify that equation (A109) holds for

$$A = \begin{bmatrix} A_1 \\ A_2 \\ A_3 \end{bmatrix}. \quad (\text{A112})$$

C.5. Asset pricing recursions

Before deriving the recursions for the numerical asset pricing computations, we derive a convenient form for the dynamics of the log surplus consumption ratio. We use e_i to denote a row vector with 1 in position i and zeros elsewhere. The matrix

$$\Sigma_M = e_1\Sigma \quad (\text{A113})$$

denotes the loading of consumption innovations onto the vector of shocks v_t , where e_1 is a basis vector with a one in the first position and zeros everywhere else. The volatility of consumption surprises equals:

$$\sigma_c^2 = \Sigma_M\Sigma_v\Sigma_M'. \quad (\text{A114})$$

To simplify notation, we define \hat{s}_t as the log deviation of surplus consumption from its steady state. The dynamics of \hat{s}_t , including the additional surplus consumption shock $\varepsilon_{s,t}$ that will later be set to zero, are:

$$\hat{s}_t = s_t - \bar{s}, \quad (\text{A115})$$

$$\hat{s}_t = \theta_0 \hat{s}_{t-1} + \theta_1 x_{t-1} + \theta_2 x_{t-2} + \varepsilon_{s,t-1} + \lambda(\hat{s}_{t-1}) \varepsilon_{c,t}, \quad (\text{A116})$$

where with an abuse of notation we write:

$$\lambda(\hat{s}_t) = \lambda_0 \sqrt{1 - 2\hat{s}_t - 1}, \hat{s}_t \leq s_{max} - \bar{s}, \quad (\text{A117})$$

$$\lambda(\hat{s}_t) = 0, \hat{s}_t \geq s_{max} - \bar{s}. \quad (\text{A118})$$

The steady-state surplus consumption sensitivity equals:

$$\lambda_0 = \frac{1}{\bar{S}}. \quad (\text{A119})$$

In our calculations of asset prices, we repeatedly substitute out expected log SDF growth, which equals:

$$E_t[m_{t+1}] = \log \beta - \gamma E_t \Delta \hat{s}_{t+1} - \gamma E_t \Delta c_{t+1}, \quad (\text{A120})$$

$$= -r_t - \frac{\gamma}{2} (1 - \theta_0) (1 - 2\hat{s}_t). \quad (\text{A121})$$

We often combine this with $r_t = \bar{r} + (e_3 - e_2 B) Z_t$ and $\hat{r}_t = (e_3 - e_2 B) Z_t$.

Including the constant, consumption growth is given by:

$$\Delta c_{t+1} = g + x_{t+1} - \phi x_t. \quad (\text{A122})$$

The steady state real short-term interest rate at $x_t = 0$ and $s_t = \bar{s}$ is the same as in [Campbell and Cochrane \(1999\)](#):

$$\bar{r} = \gamma g - \frac{1}{2} \gamma^2 \sigma_c^2 / \bar{S}^2 - \log(\beta). \quad (\text{A123})$$

The updating rule for the log surplus consumption ratio can then be written in terms of the state variables as:

$$\hat{s}_{t+1} = \hat{s}_t + E_t \Delta \hat{s}_{t+1} + \lambda(\hat{s}_t) \varepsilon_{c,t+1}, \quad (\text{A124})$$

$$= \hat{s}_t - E_t \Delta \hat{c}_{t+1} + \frac{1}{\gamma} \left(\log \beta + \hat{r}_t + \bar{r} + \frac{\gamma}{2} (1 - \theta_0) (1 - 2\hat{s}_t) \right) + \lambda(\hat{s}_t) \varepsilon_{c,t+1}, \quad (\text{A125})$$

$$= \theta_0 \hat{s}_t + \frac{1}{\gamma} (e_3 - e_2 B) A^{-1} \tilde{Z}_t - e_1 [B - \phi I] A^{-1} \tilde{Z}_t + \lambda(\hat{s}_t) \varepsilon_{c,t+1}. \quad (\text{A126})$$

C.5.1. Recursion for zero-coupon consumption claims

We now derive the recursion for zero-coupon consumption claims in terms of state variables \tilde{Z}_t , \hat{s}_t and x_{t-1} . Let P_{nt}^c / C_t denote the price-dividend ratio of a zero-coupon claim on consumption at time $t+n$. The outline of our strategy here is that we first derive an analytic expression for the price-dividend ratio for P_{1t}^c / C_t . For $n \geq 1$ we guess and verify recursively that there exists a function $F_n(\tilde{Z}_t, \hat{s}_t, x_{t-1})$, such that

$$\frac{P_{nt}^c}{C_t} = F_n(\tilde{Z}_t, \hat{s}_t, x_{t-1}). \quad (\text{A127})$$

The ex-dividend price-consumption ratio for a claim to all future consumption is then given by

$$\frac{P_t}{C_t} = F(\tilde{Z}_t, \hat{s}_t, x_{t-1}), \quad (\text{A128})$$

where we define

$$F\left(\tilde{Z}_t, \hat{s}_t, x_{t-1}\right) = \sum_{n=1}^{\infty} F_n\left(\tilde{Z}_t, \hat{s}_t, x_{t-1}\right). \quad (\text{A129})$$

We now derive the recursion of zero-coupon consumption claims in terms of state variables \tilde{Z}_t and \hat{s}_t . The one-period zero coupon price-consumption ratio solves:

$$\frac{P_{1,t}^c}{C_t} = E_t \left[\frac{M_{t+1} C_{t+1}}{C_t} \right] \quad (\text{A130})$$

We simplify

$$\frac{M_{t+1} C_{t+1}}{C_t} = \beta \exp(E_t m_{t+1} + E_t \Delta c_{t+1} - \gamma(\hat{s}_{t+1} - E_t s_{t+1}) - (\gamma - 1)(c_{t+1} - E_t c_{t+1})).$$

Using the notation $f_n = \log(F_n)$, this gives the log one-period price-consumption ratio as:

$$\begin{aligned} f_1\left(\tilde{Z}_t, \hat{s}_t, x_{t-1}\right) &= -r_t - \frac{\gamma}{2}(1 - \theta_0)(1 - 2\hat{s}_t) + g + E_t x_{t+1} - \phi x_t \\ &\quad + \frac{1}{2}(\gamma\lambda(\hat{s}_t) + (\gamma - 1))^2 \sigma_c^2, \end{aligned} \quad (\text{A131})$$

$$\begin{aligned} &= g + e_1 [B - \phi I] A^{-1} \tilde{Z}_t + \frac{1}{2}(\gamma\lambda(\hat{s}_t) + (\gamma - 1))^2 \sigma_c^2 \\ &\quad - \bar{r} - (e_3 - e_2 B) A^{-1} \tilde{Z}_t - \frac{\gamma}{2}(1 - \theta_0)(1 - 2\hat{s}_t) \end{aligned} \quad (\text{A132})$$

Next, we solve for f_n , $n \geq 2$ iteratively. Note that:

$$\frac{P_{nt}^c}{C_t} = \mathbb{E}_t \left[\frac{M_{t+1} C_{t+1}}{C_t} \frac{P_{n-1,t+1}^c}{C_{t+1}} \right] = \mathbb{E}_t \left[\frac{M_{t+1} C_{t+1}}{C_t} F_{n-1}\left(\tilde{Z}_{t+1}, \hat{s}_{t+1}, x_t\right) \right] \quad (\text{A133})$$

This gives the following expression for f_n :

$$\begin{aligned} f_n(\tilde{Z}_t, \hat{s}_t, \hat{r}_{t-1}) &= \log \left[\mathbb{E}_t \left[\exp \left(g + e_1 [B - \phi I] A^{-1} \tilde{Z}_t \right. \right. \right. \\ &\quad \left. \left. - \bar{r} - (e_3 - e_2 B) A^{-1} \tilde{Z}_t - \frac{\gamma}{2}(1 - \theta_0)(1 - 2\hat{s}_t) \right. \right. \\ &\quad \left. \left. - (\gamma(1 + \lambda(\hat{s}_t)) - 1) \sigma_c \epsilon_{1,t+1} \right. \right. \\ &\quad \left. \left. + f_{n-1}(\tilde{Z}_{t+1}, \hat{s}_{t+1}, \hat{r}_t) \right) \right]. \end{aligned} \quad (\text{A134})$$

Here, $\epsilon_{1,t+1}$ denotes the first dimension of the shock ϵ_{t+1} .

C.5.2. Recursion for zero-coupon bond prices

We use $P_{n,t}^{\$}$ and $P_{n,t}$ to denote the prices of nominal and real n -period zero-coupon bonds. The strategy is to develop analytic expressions for one- and two-period bond prices. We then guess and verify recursively that the prices of real and nominal zero-coupon bonds with maturity $n \geq 2$ can be written in the following form:

$$P_{n,t} = B_n(\tilde{Z}_t, \hat{s}_t, x_{t-1}), \quad (\text{A135})$$

$$P_{n,t}^{\$} = \exp(-n v_t^*) B_n^{\$}(\tilde{Z}_t, \hat{s}_t, x_{t-1}), \quad (\text{A136})$$

where $B_n(\tilde{Z}_t, \hat{s}_t, x_{t-1})$ and $B_n^{\$}(\tilde{Z}_t, \hat{s}_t, x_{t-1})$ are functions of the state variables. As discussed in the main paper, we assume that the short-term nominal interest rate contains no risk premium, so the one-period log nominal interest rate equals $i_t = r_t + E_t \pi_{t+1}$. Taking account of the constants, one-period bond prices

equal:

$$P_{1,t}^{\$} = \exp(-Y_{3,t} - v_t^* - \bar{r}), \quad (\text{A137})$$

$$P_{1,t} = \exp(-Y_{3,t} + \mathbb{E}_t Y_{2,t+1} - \bar{r}). \quad (\text{A138})$$

We next solve for longer-term bond prices including risk premia. Substituting in (A137) into the bond-pricing recursion gives:

$$P_{2,t}^{\$} = \mathbb{E}_t \left[M_{t+1} P_{1,t+1}^{\$} \exp(-v_{t+1}^* - Y_{2,t+1}) \right] \quad (\text{A139})$$

$$= \mathbb{E}_t \left[M_{t+1} \exp(-Y_{3,t+1} - 2v_{t+1}^* - Y_{2,t+1} - \bar{r}) \right]. \quad (\text{A140})$$

We can now verify that the two-period nominal bond price takes the form (A136):

$$\begin{aligned} B_2^{\$}(\tilde{Z}_t, \hat{s}_t, x_{t-1}) &= \exp(E_t(m_{t+1} - Y_{3,t+1} - Y_{2,t+1}) - \bar{r}) \\ &\times \mathbb{E}_t \left[\exp \left(\left(-\gamma(\lambda(\hat{s}_t) + 1) \Sigma_M - \underbrace{[(e_2 + e_3)\Sigma + 2e_4]}_{v_s} \right) v_{t+1} \right) \right]. \end{aligned} \quad (\text{A141})$$

Here, we define the vector v_s to simplify notation. The random walk component of inflation v_t^* does not appear in (A141), because $B_2^{\$}$ is already scaled by $\exp(-2v_t^*)$ by definition (A136). Taking logs, substituting out for $E_t m_{t+1}$, and using the definition for the sensitivity function $\lambda(\hat{s}_t)$, we get:

$$\begin{aligned} b_2^{\$} &= -e_3[I + B]A^{-1}\tilde{Z}_t + \frac{1}{2}v_s \Sigma_v v_s' \\ &\quad + \gamma(\lambda(\hat{s}_t) + 1) \Sigma_M \Sigma_v v_s' - 2\bar{r}. \end{aligned} \quad (\text{A142})$$

We similarly solve for two-period real bond prices in closed form:

$$\begin{aligned} P_{2,t} &= \exp(E_t(m_{t+1} - Y_{3,t+1} + Y_{2,t+2}) - \bar{r}) \\ &\times \mathbb{E}_t \left[\exp \left(\left(-\gamma(\lambda(\hat{s}_t) + 1) \Sigma_M - \underbrace{(e_3 - e_2 B)\Sigma}_{v_r} \right) v_{t+1} \right) \right] \end{aligned} \quad (\text{A143})$$

We define the vector v_r to simplify notation. Taking logs, substituting out for $E_t m_{t+1}$, and using the definition for $\lambda(\hat{s}_t)$ gives:

$$b_2(\tilde{Z}_t, \hat{s}_t, x_{t-1}) = -(e_3 - e_2 B)[I + B]A^{-1}\tilde{Z}_t + \frac{1}{2}v_r \Sigma_v v_r' + \gamma(\lambda(\hat{s}_t) + 1) \Sigma_M \Sigma_v v_r' - 2\bar{r}. \quad (\text{A144})$$

For $n \geq 3$, we repeatedly substitute out for $E_t m_{t+1}$ to obtain the following recursion for real bond prices:

$$\begin{aligned} B_n(\tilde{Z}_t, \hat{s}_t, x_{t-1}) &= \mathbb{E}_t \left[\exp \left(m_{t+1} + b_{n-1}(\tilde{Z}_{t+1}, \hat{s}_{t+1}, x_t) \right) \right] \\ &= \mathbb{E}_t \left[\exp \left(-\bar{r} - (e_3 - e_2 B)A^{-1}\tilde{Z}_t - \frac{\gamma}{2}(1 - \theta_0)(1 - 2\hat{s}_t) \right. \right. \\ &\quad \left. \left. - \gamma(1 + \lambda(\hat{s}_t))\sigma_c \epsilon_{1,t+1} + b_{n-1}(\tilde{Z}_{t+1}, \hat{s}_{t+1}, x_t) \right) \right]. \end{aligned} \quad (\text{A145})$$

The recursion for nominal bond prices with $n \geq 3$ is similar. It is complicated by the fact that we

need to integrate over $v_{LT,t+1}$, which is not necessarily spanned by ϵ_{t+1} :

$$B_n^{\mathbb{S}}(\tilde{Z}_t, \hat{s}_t, x_{t-1}) = \mathbb{E}_t \left[\exp \left(m_{t+1} - Y_{2,t+1} - nv_{t+1}^{LT} + b_{n-1}^{\mathbb{S}}(\tilde{Z}_{t+1}, \hat{s}_{t+1}, x_t) \right) \right]. \quad (\text{A146})$$

To reduce the number of dimensions along which we need to integrate numerically, we split v_{t+1}^{LT} into a component that is spanned by ϵ_{t+1} plus an orthogonal shock. This is useful because we can then use analytic expressions to integrate over the orthogonal component. We use the standard expression for conditional distributions of multivariate normal random variables. The distribution of v_{t+1}^{LT} conditional on ϵ_{t+1} is normal with:

$$v_{t+1}^{LT} | \epsilon_{t+1} \sim N \left(\underbrace{(A\Sigma\Sigma_v e'_4)'}_{vec^*} \epsilon_{t+1}, \underbrace{(\sigma_{LT})^2 - (A\Sigma\Sigma_v e'_4)'(A\Sigma\Sigma_v e'_4)}_{\sigma_{\perp}^2} \right). \quad (\text{A147})$$

We then write v_{t+1}^{LT} as the sum of two independent shocks:

$$v_{t+1}^{LT} = vec^* \epsilon_{t+1} + \epsilon_{t+1}^{\perp}, \quad (\text{A148})$$

where ϵ_{t+1}^{\perp} is defined as

$$\epsilon_{t+1}^{\perp} := v_{t+1}^{LT} - vec^* \epsilon_{t+1} \quad (\text{A149})$$

We integrate analytically over ϵ_{t+1}^{\perp} in equation (A150):

$$\begin{aligned} B_n^{\mathbb{S}}(\tilde{Z}_t, \hat{s}_t, x_{t-1}) &= \mathbb{E}_t \left[\exp \left(m_{t+1} - Y_{2,t+1} - nvec^* \epsilon_{t+1} + \frac{n^2}{2}(\sigma_{\perp})^2 + b_{n-1}^{\mathbb{S}}(\tilde{Z}_{t+1}, \hat{s}_{t+1}, B^{\mathbb{S}}x_t) \right) \right], \\ &= \mathbb{E}_t \left[\exp \left(-\bar{r} - e_3 A^{-1} \tilde{Z}_t - \frac{\gamma}{2}(1 - \theta_0)(1 - 2\hat{s}_t) \right. \right. \\ &\quad \left. \left. - (\gamma(1 + \lambda(\hat{s}_t))\sigma_c + \underbrace{e_2 A^{-1} e'_1}_{vpi_1} + nvec^* e'_1) \epsilon_{1,t+1} \right. \right. \\ &\quad \left. \left. - \left(\underbrace{e_2 A^{-1} e'_2}_{vpi_2} + nvec^* e'_2 \right) \epsilon_{2,t+1} \right. \right. \\ &\quad \left. \left. + \frac{n^2}{2}(\sigma_{\perp})^2 + b_{n-1}^{\mathbb{S}}(\tilde{Z}_{t+1}, \hat{s}_{t+1}, x_t) \right) \right]. \end{aligned} \quad (\text{A150})$$

We define the vectors vpi_1 and vpi_2 as given above to avoid computing them repeatedly in our numerical algorithm.

C.5.3. Computing returns

The log return on the consumption claim equals:

$$r_{t+1}^c = \log \left(\frac{P_{t+1}^c + C_{t+1}}{P_t^c} \right), \quad (\text{A151})$$

$$= \Delta c_{t+1} + \log \left(\frac{1 + \frac{P_{t+1}^c}{C_{t+1}}}{\frac{P_t^c}{C_t}} \right). \quad (\text{A152})$$

Real and nominal log bond yields equal:

$$y_{n,t} = -\frac{1}{n} b_{n,t}, \quad (\text{A153})$$

$$y_{n,t}^{\mathbb{S}} = -\frac{1}{n} b_{n,t}^{\mathbb{S}} + v_t^*. \quad (\text{A154})$$

Real log bond returns equal:

$$r_{n,t+1} = b_{n-1,t+1} - b_{n,t}. \quad (\text{A155})$$

Nominal log bond returns equal:

$$r_{n,t+1}^{\$} = b_{n-1,t+1}^{\$} - b_{n,t}^{\$} - (n-1)v_{t+1}^* + nv_t^*. \quad (\text{A156})$$

Real and nominal bond log excess returns then equal:

$$xr_{n,t+1} = r_{n,t+1} - r_t, \quad (\text{A157})$$

$$xr_{n,t+1}^{\$} = r_{n,t+1}^{\$} - i_t. \quad (\text{A158})$$

C.5.4. Levered stock prices and returns

We note that the price of the levered equity claim is δP_t^c , so the price-dividend ratio equals:

$$\frac{P_t^\delta}{D_t^\delta} = \delta \frac{C_t}{D_t^\delta} \frac{P_t^c}{C_t}. \quad (\text{A159})$$

Using the expression

$$D_{t+1}^\delta = P_{t+1}^c + C_{t+1} - (1-\delta)P_t^c \exp(r_t) - \delta P_t^c, \quad (\text{A160})$$

and

$$P_t^\delta = \delta P_t^c \quad (\text{A161})$$

gives the gross return on levered stocks:

$$(1 + R_{t+1}^\delta) = \frac{D_{t+1}^\delta + P_{t+1}^\delta}{P_t^\delta}, \quad (\text{A162})$$

$$= \frac{1}{\delta} \frac{P_{t+1}^c + C_{t+1} - (1-\delta)P_t^c \exp(r_t)}{P_t^c}, \quad (\text{A163})$$

$$= \frac{1}{\delta} (1 + R_{t+1}^c) - \frac{1-\delta}{\delta} \exp(r_t). \quad (\text{A164})$$

Log stock excess returns then equal:

$$xr_{t+1}^\delta = r_{t+1}^\delta - r_t. \quad (\text{A165})$$

To mimic firms' dividend smoothing in the data, we report simulated moments for the price of equities dividend by dividends smoothed over the past 64 quarters:

$$P_t^\delta / \left(\frac{1}{64} (D_t^\delta + D_{t-1}^\delta + \dots + D_{t-63}^\delta) \right). \quad (\text{A166})$$

C.6. Industry portfolio returns

We compute industry portfolio returns for industry j exactly as for the market but setting $\delta^j \neq \delta$. For each industry j we set

$$\delta^j = \frac{\delta}{\beta^j}, \quad (\text{A167})$$

where β^j is the unconditional beta obtained from regressing quarterly industry returns onto quarterly value-weighted market returns in the data for the sample 1993Q1-2019Q1.

C.7. Risk-premium decomposition

We use the superscript rn for risk-neutral, superscript cf for cash flow, and rp for risk premium. Risk-neutral valuations are expected cash flows discounted with the risk-neutral discount factor, that is consistent with equilibrium dynamics for the real interest rate:

$$M_{t+1}^{rn} = \exp(-r_t). \quad (\text{A168})$$

C.7.1. Risk-neutral zero-coupon bond prices

We use analogous recursions to solve for risk-neutral bond prices. One-period risk-neutral bond prices are given exactly as before by equations (A137) and (A138). For $n > 1$, we guess and verify that the prices of real and nominal risk-neutral zero-coupon bonds with maturity n can be written in the following form

$$P_{n,t}^{rn} = B_n^{rn}(\tilde{Z}_t, \hat{s}_t, x_{t-1}), \quad (\text{A169})$$

$$P_{n,t}^{\mathbb{S},rn} = \exp(-nv_t^*) B_n^{\mathbb{S},rn}(\tilde{Z}_t, \hat{s}_t, x_{t-1}). \quad (\text{A170})$$

for some functions $B_n^{rn}(\tilde{Z}_t, \hat{s}_t, x_{t-1})$ and $B_n^{\mathbb{S},rn}(\tilde{Z}_t, \hat{s}_t, x_{t-1})$.

We derive the two-period risk-neutral nominal bond price analytically:

$$P_{2,t}^{\mathbb{S},rn} = \exp(-r_t) \mathbb{E}_t \left[P_{1,t+1}^{\mathbb{S},rn} \exp(-v_{t+1}^* - Y_{2,t+1}) \right] \quad (\text{A171})$$

$$= \exp(-r_t) \mathbb{E}_t \left[\exp(-Y_{3,t+1} - 2v_{t+1}^* - Y_{2,t+1} - \bar{r}) \right]. \quad (\text{A172})$$

We can hence verify that the two-period risk-neutral nominal bond price takes the form (A136)

$$b_2^{\mathbb{S},rn} = -e_3 [I + B] A^{-1} \tilde{Z}_t + \frac{1}{2} v_{\mathbb{S}} \Sigma_v v_{\mathbb{S}}' - 2\bar{r} \quad (\text{A173})$$

Here, the vector $v_{\mathbb{S}}$ is identical to the case with risk aversion. Comparing expressions (A173) and (A142) shows that they agree when $\gamma = 0$. We similarly solve for 2-period real bond prices in closed form:

$$\begin{aligned} P_{2,t}^{rn} &= \exp(-Y_{3,t} + \mathbb{E}_t Y_{2,t+1} - \bar{r}) \times \exp(\mathbb{E}_t(-Y_{3,t+1} + \mathbb{E}_{t+1} Y_{2,t+2} - \bar{r})) \\ &\times \mathbb{E}_t \left[\exp \left(- \underbrace{(e_3 - e_2 B) \Sigma v_{t+1}}_{v_r} \right) \right]. \end{aligned} \quad (\text{A174})$$

The vector v_r is again identical to the case with risk aversion. Taking logs gives:

$$b_2^{rn}(\tilde{Z}_t, \hat{s}_t, x_{t-1}) = -(e_3 - e_2 B) [I + B] A^{-1} \tilde{Z}_t + \frac{1}{2} v_r \Sigma_v v_r' - 2\bar{r}. \quad (\text{A175})$$

We note that the risk-neutral bond prices (A175) and bond prices with risk aversion (A144) are identical when the utility curvature parameter γ equals zero.

For $n \geq 3$ the n -period risk neutral real bond price B_n^{rn} satisfies the recursion:

$$B_n^{rn}(\tilde{Z}_t, \hat{s}_t, x_{t-1}) = \mathbb{E}_t \left[\exp \left(-\bar{r} - (e_3 - e_2 B) A^{-1} \tilde{Z}_t + b_{n-1}(\tilde{Z}_{t+1}, \hat{s}_{t+1}, x_t) \right) \right] \quad (\text{A176})$$

We obtain a similar recursion for risk-neutral nominal bond prices:

$$B_n^{\mathbb{S},rn}(\tilde{Z}_t, \hat{s}_t, x_{t-1}) = \mathbb{E}_t \left[\exp \left(Y_{3,t} + \mathbb{E}_t Y_{2,t+1} - \bar{r} - Y_{2,t+1} - nv_{t+1}^* + b_{n-1}^{\mathbb{S}}(\tilde{Z}_{t+1}, \hat{s}_{t+1}, x_t) \right) \right].$$

We again use the decomposition $v_{t+1}^* = \text{vec}^* \epsilon_{t+1} + \epsilon_{t+1}^\perp$ from Section C.5.2 to reduce the dimensionality

of the numerical integration:

$$B_n^{s, rn}(\tilde{Z}_t, \hat{s}_t, x_{t-1}) = \mathbb{E}_t \left[\exp \left(-Y_{3,t} + \mathbb{E}_t Y_{2,t+1} - \bar{r} - Y_{2,t+1} - n \cdot \text{vec}^* \epsilon_{t+1} + \frac{n^2}{2} (\sigma^\perp)^2 + b_{n-1}^s(\tilde{Z}_{t+1}, \hat{s}_{t+1}, x_t) \right) \right], \quad (\text{A177})$$

$$= \mathbb{E}_t \left[\exp \left(-\bar{r} - e_3 A^{-1} \tilde{Z}_t - \underbrace{(e_2 A^{-1} e'_1 + n \cdot \text{vec}^* e'_1)}_{vpi_1} \epsilon_{1,t+1} - \left(\underbrace{e_2 A^{-1} e'_2 + n \cdot \text{vec}^* e'_2}_{vpi_2} \right) \epsilon_{2,t+1} + \frac{n^2}{2} (\sigma^\perp)^2 + b_{n-1}^s(\tilde{Z}_{t+1}, \hat{s}_{t+1}, x_t) \right) \right]. \quad (\text{A178})$$

C.7.2. Risk-neutral zero-coupon consumption claims

Next, we derive recursive solutions for the risk-neutral prices of zero-coupon consumption claims. Let $P_{nt}^{c, rn}/C_t$ denote the risk-neutral price-dividend ratio of a zero-coupon claim on consumption at time $t+n$. The risk-neutral price-consumption ratio of a claim to the entire stream of future consumption equals:

$$\frac{P_t^{c, rn}}{C_t} = \sum_{n=1}^{\infty} \frac{P_{nt}^{c, rn}}{C_t}. \quad (\text{A179})$$

For $n \geq 1$, we guess and verify there exists a function $F_n^{rn}(\tilde{Z}_t, \hat{s}_t, x_{t-1})$, such that

$$\frac{P_{nt}^{c, rn}}{C_t} = F_n^{rn}(\tilde{Z}_t, \hat{s}_t, x_{t-1}). \quad (\text{A180})$$

We start by deriving the analytic expression for F_1^{rn} . The one-period risk-neutral zero-coupon price-consumption ratio solves

$$\frac{P_{1,t}^{c, rn}}{C_t} = \exp(-Y_{3,t} + \mathbb{E}_t Y_{2,t+1} - \bar{r}) \mathbb{E}_t \left[\frac{C_{t+1}}{C_t} \right] \quad (\text{A181})$$

Using (A83) to substitute for consumption growth, we can derive the following analytic expression for f_1^{rn} :

$$f_1^{rn}(\tilde{Z}_t, \hat{s}_t, x_{t-1}) = -(e_3 - e_2 B) A^{-1} \tilde{Z}_t - \bar{r} + g + e_1 [B - \phi I] A^{-1} \tilde{Z}_t + \frac{1}{2} \sigma_c^2. \quad (\text{A182})$$

Next, we solve for f_n , $n \geq 2$ iteratively:

$$\frac{P_{nt}^{c, rn}}{C_t} = \exp(-Y_{3,t} + \mathbb{E}_t Y_{2,t+1} - \bar{r}) \mathbb{E}_t \left[\frac{C_{t+1}}{C_t} F_{n-1}^{rn}(\tilde{Z}_{t+1}, \hat{s}_{t+1}, x_t) \right] \quad (\text{A183})$$

This gives the following expression for f_n^{rn} :

$$f_n^{rn}(\tilde{Z}_t, \hat{s}_t, x_{t-1}) = \log \left[\mathbb{E}_t \left[\exp \left(-(Y_{3,t} + \mathbb{E}_t Y_{2,t+1}) - \bar{r} + g - \phi x_t + \mathbb{E}_t x_{t+1} + \sigma_c \epsilon_{1,t+1} + f_{n-1}^{rn}(\tilde{Z}_{t+1}, \hat{s}_{t+1}, x_t) \right) \right] \right]. \quad (\text{A184})$$

Finally, we re-write $f_{n,t}^{rn}$ as an expectation involving $f_{n-1,t+1}^{rn}$, the state variables \tilde{Z}_t , and period $t+1$

shocks:

$$f_n^{rn}(\tilde{Z}_t, \hat{s}_t, x_{t-1}) = \log \left[\mathbb{E}_t \left[\exp \left(g + e_1[B - \phi I]A^{-1}\tilde{Z}_t - \bar{r} - (e_3 - e_2B)A^{-1}\tilde{Z}_t + \right. \right. \right. \\ \left. \left. \left. + \sigma_c \epsilon_{1,t+1} + f_{n-1}^{rn}(\tilde{Z}_{t+1}, \hat{s}_{t+1}, x_t) \right) \right] \right]. \quad (\text{A185})$$

C.7.3. Risk-neutral returns

We plug risk-neutral price-consumption ratios and bond prices into equations (A152) through (A158). This gives risk-neutral returns on the consumption claim, risk-neutral log excess bond returns, and risk-neutral bond yields. We then substitute risk-neutral returns on the consumption claim into (A164)-(A165) to obtain risk-neutral log excess stock returns.

C.8. Modeling FOMC High-Frequency Asset Prices

In order to simulate high-frequency changes in stocks and bonds around FOMC announcements, we decompose the quarterly shock into a pre-FOMC and an FOMC component, which are assumed to be uncorrelated

$$v_t = v_t^{pre} + v_t^{FOMC}. \quad (\text{A186})$$

We therefore effectively model FOMC dates as occurring always at the end of the quarter, because that is the only date when we compute asset prices. The variance-covariance matrix of shocks released prior to the FOMC announcement is

$$\Sigma_v^{pre} = \Sigma_v - \text{diag}([\sigma_x^{FOMC}, \sigma_\pi^{FOMC}, \sigma_{ST}^{FOMC}, \sigma_{LT}^{FOMC}]). \quad (\text{A187})$$

We then split the rotated ϵ_t shock similarly according to

$$\epsilon_t^{pre} = A \Sigma v_t^{pre}, \quad (\text{A188})$$

$$\epsilon_t^{FOMC} = A \Sigma v_t^{FOMC}. \quad (\text{A189})$$

The aggregate dynamics and asset pricing solution are of course unchanged to before, because the distribution of quarterly fundamental shocks v_t is unchanged. But splitting it into two independent shocks allows us to differentiate asset prices before vs. after the FOMC shock v_t^{FOMC} .

We compute pre-FOMC asset prices very simply at the expected quarter t state vector before the FOMC shock is realized. The expected pre-FOMC state variables plus consumption are given by

$$\tilde{Z}_t^{pre} = \tilde{B}\tilde{Z}_{t-1} + \epsilon_t^{pre}, \quad (\text{A190})$$

$$Y_t^{pre} = BY_{t-1} + A^{-1}\epsilon_t^{pre}, \quad (\text{A191})$$

$$\hat{s}_t^{pre} = \theta_0\hat{s}_{t-1} + \theta_1Y_{1,t-1} + \theta_2Y_{1,t-2} + \dots\lambda(\hat{s}_{t-1}, \bar{S})\sigma_c\epsilon_{1,t}^{pre}, \quad (\text{A192})$$

$$c_t^{pre} = g + c_{t-1} + (Y_{1,t}^{pre} - \phi Y_{1,t-1}), \quad (\text{A193})$$

$$v_t^{*,pre} = v_{t-1}^* + v_t^{LT,pre}. \quad (\text{A194})$$

We compute pre-FOMC stock and bond prices by substituting the pre-FOMC state vector into the solutions from the asset pricing value function iterations:

$$\frac{P_t^{pre}}{C_t^{pre}} = F\left(\tilde{Z}_t^{pre}, \hat{s}_t^{pre}, x_{t-1}\right), \quad (\text{A195})$$

$$P_{n,t}^{\$,pre} = \exp(-nv_t^{*,pre}) B_n^{\$}\left(\tilde{Z}_t^{pre}, \hat{s}_t^{pre}, x_{t-1}\right), \quad (\text{A196})$$

$$P_{n,t}^{pre} = B_n\left(\tilde{Z}_t^{pre}, \hat{s}_t^{pre}, x_{t-1}\right) \quad (\text{A197})$$

The pre-FOMC nominal and real log bond yields are then given by

$$y_{n,t}^{\$,pre} = -n \log \left(P_{n,t}^{\$,pre} \right), \quad (\text{A198})$$

$$y_{n,t}^{pre} = -n \log \left(P_{n,t}^{pre} \right). \quad (\text{A199})$$

Pre-FOMC breakeven is computed as

$$breakeven_{n,t}^{pre} = y_{n,t}^{\$,pre} - y_{n,t}^{pre}. \quad (\text{A200})$$

We then compute simulated changes in the short-term nominal interest rate, as well as long-term bond yields and breakeven around FOMC announcements

$$\Delta i_t^{FOMC} = (Y_{3,t} + v_t^*) - (Y_{3,t}^{pre} + v_t^{*,pre}), \quad (\text{A201})$$

$$\Delta y_{n,t}^{\$,FOMC} = y_{n,t}^{\$} - y_{n,t}^{\$,pre}, \quad (\text{A202})$$

$$\Delta y_{n,t}^{FOMC} = y_{n,t} - y_{n,t}^{pre}, \quad (\text{A203})$$

$$\Delta breakeven_{n,t}^{FOMC} = breakeven_{n,t} - breakeven_{n,t}^{pre}. \quad (\text{A204})$$

Stock returns around the FOMC date are computed assuming that no consumption takes place during the FOMC interval (equivalently, the FOMC interval is infinitesimal), so

$$r_t^{c,FOMC} = \log \left(\exp(c_t - c_t^{pre}) \frac{\frac{P_t^c}{C_t}}{\frac{P_t^{c,pre}}{C_t^{pre}}} \right). \quad (\text{A205})$$

The levered stock market return around the FOMC date then is

$$r_t^{\delta,FOMC} = \log((1/\delta)\exp(r_t^{c,FOMC}) - ((1 - \delta)/\delta)), \quad (\text{A206})$$

which follows from using the standard formula for levered stock returns while setting the real interest rate and consumption to zero, because the FOMC interval is infinitesimal. Returns for industry j around the FOMC announcement are computed by using δ^j rather than δ in the expression (A206).

D. Solving for Asset Prices numerically

We evaluate asset prices by iterating on a grid for the state vector as in [Campbell et al. \(2020\)](#) building on [Wachter \(2005\)](#). Other numerical methodologies are faster, but their cost is that they cannot replicate the economic properties of [Wachter \(2005\)](#)'s numerical solution for Campbell-Cochrane. [Lopez, López-Salido, and Vazquez-Grande \(2018\)](#) develop an analytically convenient solution method, that approximates the sensitivity function λ by an affine function. While their method is analytically more convenient than ours, their Figure 1 shows an average price-dividend ratio of around 25 for the original Campbell and Cochrane (1999) model, whereas [Wachter \(2005\)](#)'s numerical best practices yield a price-dividend ratio of 35. Figure 1 in [Lopez, López-Salido, and Vazquez-Grande \(2018\)](#) also shows clearly that perturbation methods and global solution methods generate similarly economically meaningful differences with [Wachter \(2005\)](#)'s best practice numerical solution. In unreported results, we verified that analytic affine approximations to the sensitivity function λ (such as in [Lopez, López-Salido, and Vazquez-Grande 2015](#)), numerical higher-order perturbation methods using Dynare ([Rudebusch and Swanson 2008](#)), and global projection methods give solutions for Campbell-Cochrane that are economically very different from [Wachter \(2005\)](#)'s numerical solution. We therefore follow the practice of [Wachter \(2005\)](#) and extend the numerical grid solution to our setting with multiple state variables, which is facilitated by the log-linear dynamics of macroeconomic state variables.

Other approaches in the literature are also not appropriate for our problem. While [Chen \(2017\)](#) solves a model with habit and production using global projection and perturbation methods, his model features a linear sensitivity function and heteroskedastic consumption. [Andreasen \(2020\)](#) also uses perturbation methods for a model with heteroskedastic shocks. By contrast, we have homoskedastic consumption and

the highly nonlinear sensitivity function required to make the real risk-free rate well-behaved means that perturbation methods do not work well. Similarly, affine term structure models, such as Dai and Singleton (2000), generate affine relations between risk premia and state variables by assuming analytically convenient functional forms for the pricing kernel. In contrast to models that assume more convenient pricing kernels, our preferences are consistent with the standard log-linear New Keynesian consumption Euler equation and generate conditionally homoskedastic macroeconomic dynamics.

While iterating on a grid is significantly slower than perturbation or global projection methods, it is not prohibitively so, taking about 2minutes on a standard laptop.

D.1. Implementing the asset pricing recursions

We implement the recursions in Sections C.5.1 and C.5.2 numerically through value function iteration on a grid. We solve for the functions f_n , b_n , and b_n^s using value function iteration along a five-dimensional state vector. We use a five-dimensional grid, with the first three dimensions corresponding to \tilde{Z}_t , the fourth dimension corresponding to \hat{s}_t , and the fifth dimension corresponding to x_{t-1} .

D.1.1. Grid

In this Section, we use \tilde{Z}, \hat{s}, x to denote the corresponding time- t variables. We use superscripts $-$ to denote variables in the previous period and $+$ to denote variables in the next period. We solve numerically for f_n , b_n , and b_n^s as functions of the vector of state variables $[\tilde{Z}, \hat{s}, x^-]$.

Our grid is densest along the \hat{s} dimension to capture important non-linearities of asset prices with respect to the surplus consumption ratio. Following Wachter (2005), we choose a grid for the surplus consumption ratio that consists of an upper segment and a lower segment and covers a wide range of values for s_t . Let $S_{grid,1}$ denote a vector of 20 equally spaced points between 0 and S_{max} with S_{max} included and $s_{grid,2}$ a vector of 30 equally spaced points between $\min(\log(S_{grid,1}))$, and -50 . The grid for $\hat{s}_t = s_t - \bar{s}$ then consists of the concatenation of $s_{grid,2} - \bar{s}$ and $\log(S_{grid,1}) - \bar{s}$.

We find that bond and stock prices are close to loglinear in \tilde{Z} and \hat{x}^- , so coarser grids are sufficient along those dimensions of the state vector. In fact, the analytic expressions for f_1 , b_2 , and b_2^s show that one-period zero-coupon consumption claims and two-period bond prices are exactly log-linear in \tilde{Z} and x^- . Numerical results indicate that this property translates to longer-period claims and f_n , b_n , and b_n^s are still approximately linear in \tilde{Z} and x^- for general n . To speed up the value function iteration, we therefore use two grid points for each dimension of \tilde{Z} and for x^- .

For \tilde{Z} , we use an equal-spaced three-dimensional grid. Let N denote the number of grid points along each dimension and m the width of the grid as a multiple of the unconditional standard deviation of \tilde{Z} . For each dimension of \tilde{Z} , we choose a grid of N equal-spaced points with the lowest point equal to $-m \times std(\tilde{Z})$ and the highest point equal to $m \times std(\tilde{Z})$. Here, the unconditional variance-covariance matrix of \tilde{Z} is determined implicitly by the equation:

$$std(\tilde{Z}) = \sqrt{\tilde{B}Var(\tilde{Z})\tilde{B}' + diag(1, 1, 1)}. \quad (\text{A207})$$

For our baseline grid, we set $N = 2$ and $m = 2$.

For x^- , we consider an equal-spaced grid with $sizexm$ points ranging from $\min(e_1 A \tilde{Z}_t : \tilde{Z} \in grid)$ to $\max(e_1 A \tilde{Z}_t : \tilde{Z} \in grid)$. This choice of grid ensures that the grid for x^- covers the entire range of output gap values implied by the grid for \tilde{Z} . In our baseline evaluation, we set $sizexm = 2$.

With $N = 2$ grid points along each of the three dimensions of \tilde{Z} , 50 gridpoints for \hat{s} , and $sizexm = 2$ grid points for x^- , the combined grid has a total of $2^3 \cdot 50 \cdot 2 = 800$ points.

D.1.2. Numerical integration

Following Wachter (2005), we use Gauss-Legendre quadrature to evaluate the expectations (A134), (A145), and (A150) numerically. Gauss-Legendre quadrature is orders of magnitude faster than computing expectations by simulation. As in Wachter (2005), we evaluate infinite integrals over the density of standardized consumption shocks $(\epsilon_{1,t})$ using 40 integration node points and an integration

domain ranging from -8 standard deviations to $+8$ standard deviations. To conserve speed and memory, we integrate over shocks orthogonal to surplus consumption ($\epsilon_{2,t}$) using a somewhat smaller number of integration node points, 15, but again an integration domain of ± 8 standard deviations. To evaluate bond and stock prices at points that are not on the grid, we use loglinear multi-linear interpolation and extrapolation.

For completeness, we recap the key features of Gauss-Legendre integration. Let xGL_i , $i = 1, \dots, N_{GL}$ and $wGL_i = 1, \dots, N_{GL}$ denote the Gauss-Legendre nodes and weights of N_{GL} th order. Gauss-Legendre quadrature then approximates a definite integral of any smooth function f on the interval $[-1, 1]$ by $\int_{-1}^1 f(x) dx \approx \sum_{i=1}^{N_{GL}} wGL_i f(xGL_i)$. By change of variable, it is immediate that we can approximate the integral of a smooth function f on an interval $[-\bar{a}, \bar{a}]$ by

$$\int_{-\bar{a}}^{\bar{a}} f(x) dx \approx \sum_{i=1}^{N_{GL}} \underbrace{\bar{a} \times wGL_i}_{wGL_i^{\bar{a}}} f\left(\underbrace{\bar{a} \times xGL_i}_{xGL_i^{\bar{a}}}\right). \quad (\text{A208})$$

Here, we use $xGL_i^{\bar{a}}$ and $wGL_i^{\bar{a}}$ to denote Gauss-Legendre node points and weights scaled to the interval $[-\bar{a}, \bar{a}]$.

We implement Gauss-Legendre quadrature to take expectations over ϵ_{t+1} as follows. Let N_1 denote the number of Gauss-Legendre nodes and \bar{a}_1 denote the integration domain for the shock $\epsilon_{1,t}$, that is perfectly correlated with output innovations. We set $xGL_{1,i} = xGL_i^{\bar{a}_1}$ and $wGL_{1,i} = wGL_i^{\bar{a}_1}$ for $i = 1, \dots, N_1$, where the weights and nodes are as defined in equation (A208). Moreover, we set

$$pGL_{1,i} = \frac{1}{\sqrt{2\pi}} \exp(-xGL_{1,i}^2) wGL_{1,i} / \sum_{i=1}^{N_1} \left(\frac{1}{\sqrt{2\pi}} \exp(-xGL_{1,i}^2) wGL_{1,i} \right), \quad (\text{A209})$$

and use the scaled weights $pGL_{1,i}$ for numerical integration. The scaling of (A209) ensures that the numerical expectation of a constant is evaluated to be the same constant (or intuitively that discretized probabilities sum to one).

We then evaluate numerically the expectation of any smooth function f of $\epsilon_{1,t}$ via:

$$E[f(\epsilon_{1,t})] = \int_{-\infty}^{\infty} \frac{1}{\sqrt{2\pi}} \exp(-\epsilon_1^2) f(\epsilon_1) d\epsilon_1, \quad (\text{A210})$$

$$\approx \int_{-\bar{a}_1}^{\bar{a}_1} \frac{1}{\sqrt{2\pi}} \exp(-\epsilon_1^2) f(\epsilon_1) d\epsilon_1, \quad (\text{A211})$$

$$\approx \sum_{i=1}^{N_1} pGL_{1,i} f(xGL_{1,i}). \quad (\text{A212})$$

Accuracy increases with \bar{a}_1 and N_1 . We follow Wachter (2006) in setting $N_1 = 40$ and $\bar{a}_1 = 8$.

To take expectations over $\epsilon_{2,t}$ and $\epsilon_{3,t}$, we similarly use Gauss-Legendre quadrature with integration domain $\bar{a}_2 = 8$ and number of nodes $N_2 = 15$. We set $xGL_{2,i} = xGL_i^{\bar{a}_2}$ and $wGL_{2,i} = wGL_i^{\bar{a}_2}$ for $i = 1, \dots, N_2$ and define the scaled weights:

$$pGL_{2,i} = \frac{1}{\sqrt{2\pi}} \exp(-xGL_{2,i}^2) wGL_{2,i} / \sum_{i=1}^{N_2} \left(\frac{1}{\sqrt{2\pi}} \exp(-xGL_{2,i}^2) wGL_{2,i} \right), \quad (\text{A213})$$

The weights and nodes for $\epsilon_{3,t}$ are identical to those of $\epsilon_{2,t}$.

Since $\epsilon_{1,t}$, $\epsilon_{2,t}$, and $\epsilon_{3,t}$ are independent, we can evaluate the expectation of any smooth function

$f(\epsilon_{1,t}, \epsilon_{2,t}, \epsilon_{2,t})$ as

$$\begin{aligned}
Ef(\epsilon_{1,t}, \epsilon_{2,t}, \epsilon_{3,t}) &= \int_{-\infty}^{\infty} \frac{1}{\sqrt{2\pi}} \exp(-\epsilon_1^2) \int_{-\infty}^{\infty} \frac{1}{\sqrt{2\pi}} \exp(-\epsilon_2^2) \int_{-\infty}^{\infty} \frac{1}{\sqrt{2\pi}} \exp(-\epsilon_3^2) f(\epsilon_1, \epsilon_2, \epsilon_3) d\epsilon_1 d\epsilon_2 d\epsilon_3, \\
&\approx \sum_{i=1}^{N_1} pGL_{1,i} \left[\sum_{j=1}^{N_2} pGL_{2,j} \left[\sum_{k=1}^{N_3} pGL_{3,k} f(xGL_{1,i}, xGL_{2,j}, xGL_{3,k}) \right] \right]. \tag{A214}
\end{aligned}$$

D.1.3. Recursive step

Let a superscript num denote the numerical counterparts to the analytic functions f_n , b_n , b_n^s . We start by initializing $f_1^{num}(\tilde{Z}, \hat{s}, x^-)$, $b_2^{num}(\tilde{Z}, \hat{s}, x^-)$, and $b_2^{s,num}(\tilde{Z}, \hat{s}, x^-)$ at each grid point according to the analytic expressions (A132), (A142) and (A144).

Next, we apply the recursive expressions (A134), (A145), and (A150) along the grid. Having computed f_{n-1}^{num} along the entire grid, we evaluate $f_n^{num}(\tilde{Z}, \hat{s}, x^-)$ at a grid point $(\tilde{Z}, \hat{s}, x^-)$ as follows. We compute the expectation (A134) numerically as:

$$\begin{aligned}
f_n^{num}(\tilde{Z}, \hat{s}, x^-) &= \log \left[\sum_{i=1}^{N_1} pGL_{1,i} \left[\sum_{j=1}^{N_2} pGL_{2,j} \left[\sum_{k=1}^{N_3} pGL_{3,k} \cdot \exp \left(g + e_1 [B - \phi I] A^{-1} \tilde{Z} \right. \right. \right. \right. \\
&\quad \left. \left. \left. - \bar{r} - (e_3 - e_2 B) A^{-1} \tilde{Z} - \frac{\gamma}{2} (1 - \theta_0) (1 - 2\hat{s}) \right. \right. \right. \\
&\quad \left. \left. \left. - (\gamma(1 + \lambda(\hat{s})) - 1) \sigma_c \times xGL_{1,i} \right. \right. \right. \\
&\quad \left. \left. \left. + f_{n-1}^{num} \left(\tilde{B} \tilde{Z} + \begin{bmatrix} xGL_{1,i} \\ xGL_{2,j} \\ xGL_{3,k} \end{bmatrix}, \theta_0 \hat{s} + \theta_1 x + \theta_2 x^- + \lambda(\hat{s}) xGL_{1,i}, x \right) \right] \right] \right], \tag{A215}
\end{aligned}$$

where we evaluate x as a function of the state vector as

$$x = e_1 A^{-1} \tilde{Z}. \tag{A216}$$

To compute the right-hand-side of (A215), we need to evaluate f_{n-1}^{num} at points that are not on our grid. We interpolate f_{n-1}^{num} linearly (and hence F_{n-1}^{num} log-linearly). When the argument is outside the range of the grid, we extrapolate f_{n-1}^{num} linearly. It is clear from (A132) that linear inter- and extrapolation gives a good approximation of f_1 . In fact, we can see that f_1 is exactly linear in \tilde{Z} , independent of x^- , and that it depends on $\lambda(\hat{s}) = \lambda_0 \sqrt{1 - 2\hat{s}}$. We accommodate the fact that f_1 is not linear in \hat{s} by choosing a much denser grid along the \hat{s} dimension. We do not have analytic expressions for f_n , $n > 1$ (after all, that's why we need a numerical solution), but numerical solutions indicate that linear inter- and extrapolation gives good approximations for f_n with the chosen grid.

In terms of coding (A215), we face a trade-off between speed and readability of the code. We pre-allocate matrices outside loops and we code linear interpolation by hand (rather than using a pre-written interpolation routine) to conserve speed and memory. We also inline the linear interpolation steps (i.e. write them directly into the main function rather than calling a separate interpolation function). This speeds up the code substantially, while reducing its readability.

There are different methods to interpolate multidimensional functions. Specifically, we use multi-linear interpolation, corresponding to interpolating along each dimension one at a time. In order to enhance computational speed we do not rely on a pre-programmed interpolation routine, instead coding our own minimal interpolation routine. It is well-known that the result of multi-linear (or in the two-dimensional case bi-linear) interpolation does not depend on in which order one interpolates the different arguments. We find it convenient to interpolate $f_{n-1}^{num}(\tilde{Z}, \hat{s}, x^-)$ first along the x^- dimension, then along \hat{s} , then along \tilde{Z}_1 , and finally along the \tilde{Z}_2 and \tilde{Z}_3 dimensions.

Finally, we evaluate the price-consumption ratio for the aggregate consumption stream by

approximating it as the sum of the first 300 zero-coupon consumption claims:

$$F^{num}(\tilde{Z}_t, \hat{s}_t, x_{t-1}) = \sum_{n=1}^{300} \exp\left(f_n^{num}(\tilde{Z}_t, \hat{s}_t, x_{t-1})\right). \quad (\text{A217})$$

We iterate $b_n^{num}(\tilde{Z}, \hat{s}, x^-)$ and $b_n^{\$,num}(\tilde{Z}, \hat{s}, x^-)$ similarly according to:

$$\begin{aligned} b_n^{num}(\tilde{Z}_t, \hat{s}_t, x_{t-1}) = & \log \left[\sum_{i=1}^{N_1} pGL_{1,i} \left[\sum_{j=1}^{N_2} pGL_{2,j} \left[\sum_{k=1}^{N_3} pGL_{3,k} \right. \right. \right. \\ & \cdot \exp\left(-\bar{r} - (e_3 - e_2 B) A^{-1} \tilde{Z} - \frac{\gamma}{2}(1 - \theta_0)(1 - 2\hat{s}) \right. \\ & \left. \left. \left. - \gamma(1 + \lambda(\hat{s})) \sigma_c \times xGL_{1,i} \right. \right. \right. \\ & \left. \left. \left. + b_{n-1}^{num} \left(\tilde{B} \tilde{Z} + \begin{bmatrix} xGL_{1,i} \\ xGL_{2,j} \\ xGL_{3,k} \end{bmatrix}, \theta_0 \hat{s} + \theta_1 x + \theta_2 x^- + \lambda(\hat{s}) xGL_{1,i}, x \right) \right) \right] \right] \right], \end{aligned} \quad (\text{A218})$$

and

$$\begin{aligned} b_n^{\$,num}(\tilde{Z}_t, \hat{s}_t, x_{t-1}) = & \log \left[\sum_{i=1}^{N_1} pGL_{1,i} \left[\sum_{j=1}^{N_2} pGL_{2,j} \left[\sum_{k=1}^{N_3} pGL_{3,k} \right. \right. \right. \\ & \cdot \exp\left(-\bar{r} - e_3 A^{-1} \tilde{Z} - \frac{\gamma}{2}(1 - \theta_0)(1 - 2\hat{s}) \right. \\ & \left. \left. \left. - (\gamma(1 + \lambda(\hat{s})) \sigma_c + vpi_1 + n \cdot \text{vec}^* e'_1) \times xGL_{1,i} \right. \right. \right. \\ & \left. \left. \left. - (vpi_2 + n \cdot \text{vec}^* e'_2) xGL_{2,j} + \frac{n^2}{2} (\sigma^\perp)^2 \right. \right. \right. \\ & \left. \left. \left. + b_{n-1}^{\$,num} \left(\tilde{B} \tilde{Z} + \begin{bmatrix} xGL_{1,i} \\ xGL_{2,j} \\ xGL_{3,k} \end{bmatrix}, \theta_0 \hat{s} + \theta_1 x + \theta_2 x^- + \lambda(\hat{s}) xGL_{1,i}, x \right) \right) \right] \right] \right], \end{aligned} \quad (\text{A220})$$

We again use multi-linear interpolation and extrapolation to evaluate $b_{n-1}^{\$,num}$ and b_{n-1}^{num} at points that are not on the grid. We similarly implement the recursions (A176), (A178), and (A185) numerically to obtain risk-neutral bond and consumption claim valuations $B_n^{rn,num}$, $B_n^{rn,\$,num}$, $C^{rn,num}$.

D.2. Simulating the Model

We simulate a draw of length T . Model results in Tables 3, 4, 5, 6, and 7 use $T = 10000$ and discard the first 100 simulation periods to ensure that the system has reached the stochastic steady-state.

We use superscript *sim* to denote simulated quantities. We use the MATLAB function `mvnrnd` to obtain independent draws $v_t^{sim} \sim N(0, \Sigma_v)$ for $t = 1, 2, \dots, T$. We then obtain the rotated shock according to $\epsilon_t^{sim} = A \Sigma v_t^{sim}$ and $v_t^{LT,sim} = e_4 \Sigma v_t^{sim}$. We generate draws for $\tilde{Z}_t^{sim}, t = 1, \dots, T$ by setting $\tilde{Z}_1^{sim} = 0$ and then updating according to (A107). We obtain the simulated non-rotated state vector for $t = 1, 2, \dots, T$ through the relation $Y_t^{sim} = A^{-1} \tilde{Z}_t^{sim}$. We generate draws for the surplus consumption ratio by setting $\hat{s}_1^{sim} = 0$ and $x_0^{sim} = 0$ and then updating according to (A116). We generate the simulated random walk component of inflation $v_t^*, t = 1, 2, \dots, T$ by starting from $v_1^{*sim} = 0$ and updating it according to equation (A100). We initialize simulated log consumption at $c_1^{sim} = 0$ and update it using (A83). We then drop the first 100 simulation periods to allow the system to converge to the stochastic steady-state.

Having generated draws for the five state variables \tilde{Z}^{sim} , \hat{s}^{sim} , and x_{t-1}^{sim} , we obtain the simulated consumption-claim price-dividend ratio as $(P^c/C)_t^{sim} = F^{num}(\tilde{Z}_t^{sim}, \hat{s}_t^{sim}, x_{t-1}^{sim})$, n -period real bond

prices as

$$P_{n,t}^{sim} = B_n^{num} \left(\tilde{Z}_t^{sim}, \hat{s}_t^{sim}, x_{t-1}^{sim} \right), \text{ and}$$

$B_{n,t}^{\$,sim} = B_n^{\$,num} \left(\tilde{Z}_t^{sim}, \hat{s}_t^{sim}, x_{t-1}^{sim} \right)$. We obtain the corresponding risk-neutral valuation ratios by plugging into the risk-neutral asset pricing solutions:

$$(P^c/C)_t^{rn,sim} = F^{rn,num} \left(\tilde{Z}_t^{sim}, \hat{s}_t^{sim}, x_{t-1}^{sim} \right),$$

$$P_{n,t}^{rn,sim} = B_n^{rn,num} \left(\tilde{Z}_t^{sim}, \hat{s}_t^{sim}, x_{t-1}^{sim} \right), \text{ and}$$

$B_{n,t}^{rn,\$,sim} = B_n^{rn,\$,num} \left(\tilde{Z}_t^{sim}, \hat{s}_t^{sim}, x_{t-1}^{sim} \right)$. We obtain nominal bond prices $P_{n,t}^{\$,sim}$ by combining $B_{n,t}^{\$,sim}$ and v_t^{*sim} according to (A136). We similarly obtain risk-neutral nominal bond prices $P_{n,t}^{rn,\$,sim}$ by combining $B_{n,t}^{rn,\$,sim}$ and v_t^{*sim} according to (A136).

To deal with the fact that $\tilde{Z}_t^{sim}, \hat{s}_t^{sim}, x_{t-1}^{sim}$ are not usually on grid points we adopt a similar linear interpolation strategy as in the numerical evaluation of the asset pricing recursions described in Section D.1.3. We interpolate F^{num}, B_n^{num} , and $B_n^{\$,num}$ log-linearly. We simplify the interpolation strategy slightly compared to Section D.1.3. We use the MATLAB function `griddedInterpolant`, sacrificing some computational speed for simpler code. Even though rare events (and especially extremely negative realizations for \hat{s}) matter for the value function iteration in Section D.1.3, low-probability events have very little impact on the properties of simulated asset prices taking as given F^{num}, B_n^{num} , and $B_n^{\$,num}$. We therefore simplify the log-linear interpolation by truncating $\tilde{Z}_t^{sim}, \hat{s}_t^{sim}$, and x_{t-1}^{sim} at the maximum and minimum values covered by the grid.

Having generated $\left(\frac{P^c}{C}\right)_t^{sim}, t = 1, \dots, T$, we compute log returns on the consumption claim $r_{t+1}^{c,sim}$ according to (A152). We obtain simulated price-dividend ratios for levered stocks by plugging into (A159). Finally, we obtain log bond yields and stock and bond excess returns as described in Section C.5.3. Risk-neutral bond and stock returns are computed by substituting $\left(\frac{P^c}{C}\right)^{rn,sim}, P_{n,t}^{rn,\$,sim}$, and $P_{n,t}^{rn,sim}$ into the same relations.

We simulate pre-FOMC asset prices as follows. We use the MATLAB function `mvnrnd` to generate independent draws for the FOMC shock $v_t^{FOMC,sim} \sim N \left(0, \text{diag} \left(\left[0, 0, (\sigma_{ST}^{FOMC})^2, (\sigma_{LT}^{FOMC})^2 \right] \right) \right)$, where $t = 1, \dots, T$. Having drawn the FOMC shock $v_t^{FOMC,sim}$ we obtain the simulated pre-FOMC component of the overall quarterly simulated shock as

$$v_t^{pre,sim} = v_t^{sim} - v_t^{FOMC,sim}, \quad (\text{A221})$$

$$\epsilon_t^{pre,sim} = A \Sigma v_t^{pre,sim}. \quad (\text{A222})$$

We then use the simulated values for $\tilde{Z}_{t-1}^{sim}, Y_{t-1}^{sim}, c_{t-1}^{sim}, \hat{s}_{t-1}^{sim}, v_{t-1}^*$ and $\epsilon_t^{pre,sim}$ to compute the simulated pre-FOMC state vector according to equations (A190) through (A194). We then obtain pre-FOMC asset prices by substituting the simulated pre-FOMC state vector into equations (A195) through (A194). Simulated yield changes around FOMC news are then computed according to equations (A201) and (A204) and simulated FOMC stock returns are obtained according to equation (A206). Quarterly and high-frequency returns for industry j are generated analogously to market returns but using δ^j instead of δ .

D.3. Parameter units

This subsection details the relation between parameter values in empirical (reported in the paper) and natural units (used for solving the code). We solve the model in natural units. However, it is most natural to report empirical moments and summary statistics in empirical units for interpretability.

For comparability with empirical moments, Table 1 reports model parameters in units that correspond to the output gap in annualized percent, and inflation and interest rates in annualized percent. As in Campbell et al. (2020), we report the discount rate and the persistence of surplus consumption in annualized units. Concretely, Table 1 reports the following scaled parameters (for completeness we also list parameters where natural and empirical units are the same):

$400 \times g,$	(A223)
$\gamma,$	(A224)
$400 \times \bar{r},$	(A225)
$\theta_0^4,$	(A226)
$\theta_1,$	(A227)
	(A228)
$4 \times \gamma^x,$	(A229)
$\rho_i,$	(A230)
$400 \times \sigma_{MP},$	(A231)
$\phi,$	(A232)
δ	(A233)

Table 2 lists the following scaled implied parameter values

$\beta^4,$	(A234)
$\bar{S},$	(A235)
$S_{max},$	(A236)
$\rho^x,$	(A237)
$f^x,$	(A238)
$\frac{1}{4} \times \psi,$	(A239)
$\theta_2.$	(A240)

D.4. Switching off shocks and PC slope in numerical solution

To switch off the shocks we don't need, we set the following near-zero values for the standard deviations of the demand, Phillips curve, and long-term inflation target (random walk) shocks. The exact numerical values are chosen so that the solution remains invertible, but has converged as the shock volatilities approach zero:

$$\sigma_x = 10^{-9}, \quad (\text{A241})$$

$$\sigma_{PC} = 10^{-9}, \quad (\text{A242})$$

$$\sigma_{LT} = 10^{-9}. \quad (\text{A243})$$

We set the slope of the Phillips curve to $\kappa = 2.455710^{-5}$. To ensure that the numerical solutions work, we need to choose a value for $\rho_\pi = 0.508$. We have verified that the exact parameter values for σ_x , σ_{PC} , and σ_{LT} , κ and ρ_π do not matter for the asset pricing moments. We have also checked that the asset pricing moments for real and nominal bonds at these parameter values are identical, so the asset prices seem to have converged as the volatilities of these no-longer needed shocks converge to zero.

E. Additional Model Results

E.1. Comparative Statics by θ_1

In this Section, we complement Figure 2 by reporting quarterly stock returns and macroeconomic moments for different value for the habit parameter θ_1 . Our baseline calibration corresponds to $\theta_1 = -0.90$, while the [Campbell and Cochrane \(1999\)](#) preferences correspond to $\theta_1 = 0$. In the top panel of Table A1, we report the habit coefficients θ_1 . The parameter θ_2 is chosen according to equation (16).

The second panel in Table A1 shows quarterly moments of model stock returns. We see that the equity premium, equity volatility, persistence of price-dividend ratio, and stock return predictability are

almost completely unaffected by varying θ_1 . The final panel shows macroeconomic moments. As in Figure 2, we see that the habit parameter θ_1 matters for output response to a monetary policy shock. In particular, we need $\theta_1 = -0.90$ to match the lag and size of the trough output response to a monetary policy shock in the data.

Table A1 Quarterly Asset Prices for Different Habit Parameter Values

Parameters				Model: Varying θ_1						
θ_1	Data	-0.99	-0.95	Baseline	-0.90	-0.70	-0.50	-0.30	-0.10	CC99
Stocks										
Equity premium	7.84	7.23	7.26	7.29	7.39	7.46	7.51	7.55	7.56	
Volatility	16.87	14.75	14.81	14.87	15.09	15.25	15.36	15.45	15.48	
Sharpe Ratio	0.47	0.49	0.49	0.49	0.49	0.49	0.49	0.49	0.49	
AR(1) Coeff. pd	0.92	0.93	0.93	0.93	0.93	0.93	0.93	0.93	0.93	
1-YR Excess Returns on pd	-0.38	-0.34	-0.34	-0.34	-0.34	-0.33	-0.33	-0.33	-0.33	
1-YR Excess Returns on pd (R^2)	0.23	0.07	0.07	0.07	0.07	0.07	0.07	0.07	0.07	
Macroeconomic Dynamics										
Std. Annual Consumption Growth	1.5	1.57	1.57	1.55	1.44	1.29	1.15	1.04	1.00	
Std. Annual Change fed funds Rate	1.35	2.16	2.14	2.13	2.07	2.04	2.03	2.03	2.03	
Trough Output Response to 100 bps FF Shock	-0.7	-0.74	-0.73	-0.71	-0.64	-0.57	-0.51	-0.51	-0.52	
Lag Trough Output Response	4	5	4	4	3	2	2	1	1	

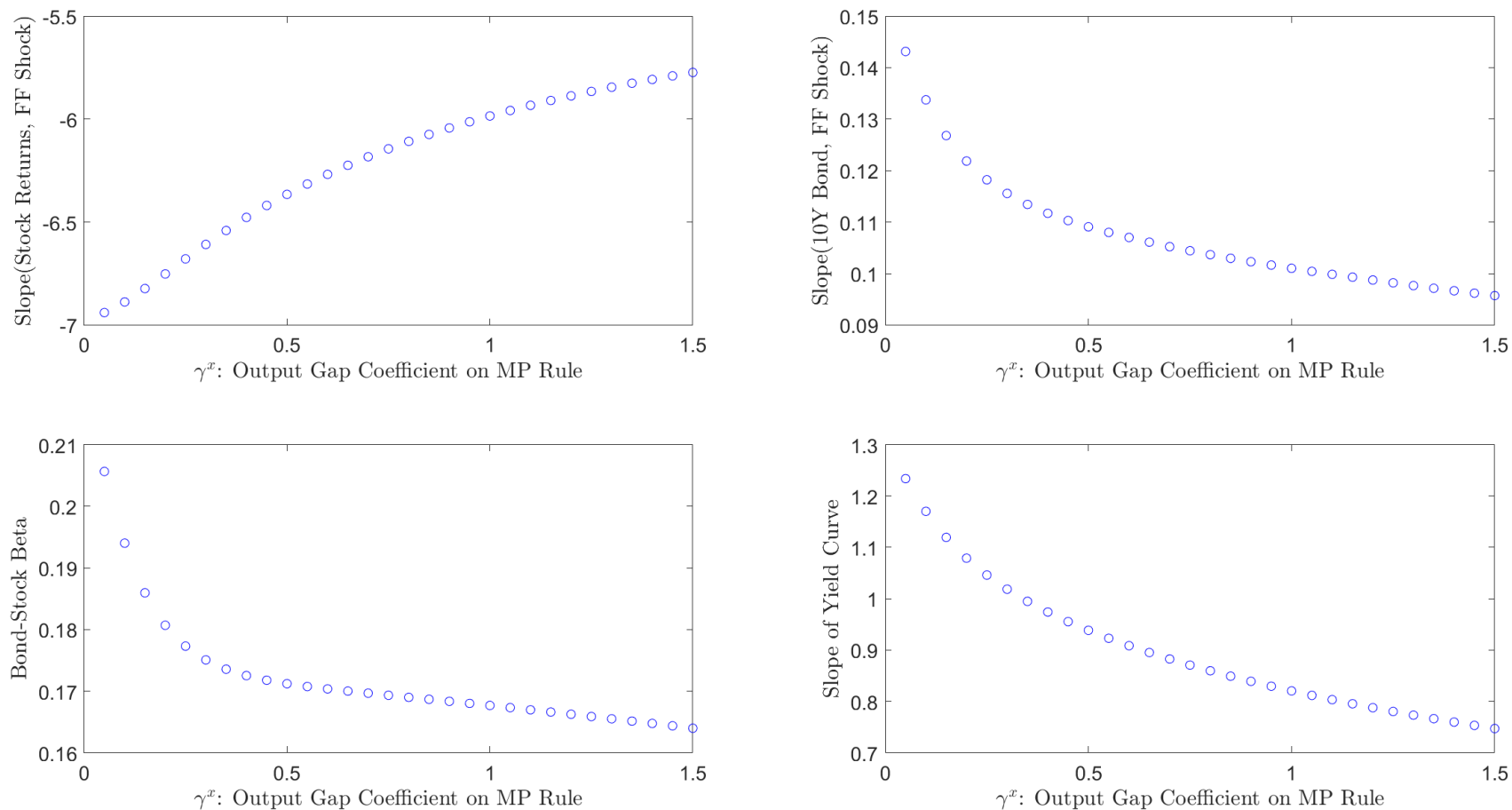
Note: This table solves for quarterly stock return moments and macroeconomic moments at different values for the habit parameter θ_1 . Our baseline calibration, reported in Table 3 in the main paper, corresponds to $\theta_1 = -0.90$. Campbell and Cochrane (1999, CC99) preferences correspond to $\theta_1 = \theta_2 = 0$. For any value of θ_1 , the parameter θ_2 is determined via equation (16) in the main paper.

E.2. Comparative statics by monetary policy rule parameter

In this Section we illustrate comparative statics of our key results across different values for the monetary policy rule parameter γ^x . Figure A1 plots key calibration outcomes on the y-axis against the monetary policy rule parameter γ^x on the x-axis. Each dot corresponds to a separate model calibration with a different parameter value for γ^x . All other parameters are held constant at their baseline values.

The top-left panel shows our benchmark regression coefficient of stock returns onto model high-frequency monetary policy shocks, exactly as in Table 4 in the main paper. The top-right panel shows the regression coefficient of 10-year nominal bond yields onto model high-frequency monetary policy shocks (as in column (2) of Table 7 in the main paper). We see that the stock and nominal bond yield responses to monetary policy shocks are strong across a very wide range of values γ^x , so our benchmark high-frequency model results are robust.

Fig. A1 Model Bond and Stock Responses to Monetary Policy Shocks - Against Monetary Policy Parameter γ_x



32

Note: This figure shows the effects of varying the output gap coefficient in the monetary policy rule, γ^x , on the regression coefficient of stock returns on the fed funds surprise (as in column 4 of Table 4 in the main paper), the regression coefficient of 10-year nominal bond yields on the fed funds surprise (as in column (1) of Table 7 in the main paper), the 10-year nominal bond-stock beta, and the slope of the nominal yield curve. Parameter γ^x ranges from 0.05 to 1.50 (30 grid points). The Phillips curve slope is held constant at $\kappa = 0$ throughout. For each parameter value, asset pricing moments are computed from a simulation of length 10,000.

E.3. Model Robustness: Larger volatility of FOMC surprises

In this Section, we verify that all our main model results are unchanged if we increase the volatility of FOMC date shocks by an order of magnitude. In this Section, we show results with $\sigma_{MP}^{FOMC} = 4.65bps = 0.0465\%$, which is somewhat smaller than the value used in the main paper of $6.52bps$, and the much the larger value $\sigma_{MP}^{FOMC} = 46.5bps = 0.465\%$.

Table A2 compares the model stock return regressions with these different values for the volatility of FOMC date shocks. All results are numerically almost identical. The only difference to note is that with $\sigma_{MP}^{FOMC} = 46.5bps$ the model implies a larger coefficient on $FF\ Shock \times (FF\ Shock > 0)$, i.e. the effect of monetary policy shocks is somewhat more asymmetric. This is as expected, since risk premia in the model are convex in consumption shocks but differentiable (i.e. locally linear) when shocks are small. Table A3 shows that the state-contingency of stock responses and bond yield responses are also unchanged when we increase σ_{MP}^{FOMC} by a full order of magnitude. We therefore conclude that our calibration results are largely insensitive to this parameter within a reasonable range.

Table A2 Stock Market onto High-Frequency Monetary Policy Shocks – Larger FOMC Date Shocks

Baseline Model: $\sigma_{MP}^{FOMC} = 6.52$		
FF Shock	-6.37	-6.31
FF Shock \times (FF Shock >0)		-0.07
Robustness Check: $\sigma_{MP}^{FOMC} = 4.65$		
FF Shock	-6.37	-6.31
FF Shock \times (FF Shock >0)		-0.06
Robustness Check: $\sigma_{MP}^{FOMC} = 46.5$		
FF Shock	-6.37	-6.13
FF Shock \times (FF Shock >0)		-0.44

Note: This table shows model robustness for Table 4 in the main paper, but uses different volatilities of FOMC date shocks σ_{MP}^{FOMC} . For comparison, the main results in Table 4 use $\sigma_{MP}^{FOMC} = 6.52bps$. We show model regressions of the form $r_{mkt,t}^{FOMC} = b_{mkt,0} + b_{mkt,1}\Delta^{FOMC}i_t + \varepsilon_{mkt,t}$, where $r_{mkt,t}^{FOMC}$ is the high-frequency stock market around of FOMC announcements. Model data is obtained from a simulation of length 10,000.

Table A3 Stock Returns onto High-Frequency Monetary Policy Shocks by Risk Aversion – Larger FOMC Date Shocks

	Mkt	Utils	NoDur	Hlth	Enrgy	Shops	Telcm	Manuf	Other	Durbl	HiTec
Baseline Model: $\sigma_{MP}^{FOMC} = 6.52$											
FF Shock	-5.39	-2.43	-3.5	-3.5	-3.94	-4.47	-5.12	-5.28	-5.61	-6.69	-7.49
FF Shock $\times (RA_t > \text{Median})$	-1.97	-0.89	-1.28	-1.28	-1.44	-1.64	-1.87	-1.93	-2.05	-2.44	-2.74
Robustness Check: $\sigma_{MP}^{FOMC} = 4.65$											
FF Shock	-5.39	-2.43	-3.5	-3.5	-3.94	-4.47	-5.12	-5.28	-5.61	-6.69	-7.49
FF Shock $\times (RA_t > \text{Median})$	-1.97	-0.89	-1.28	-1.28	-1.44	-1.64	-1.87	-1.93	-2.05	-2.44	-2.74
Robustness Check: $\sigma_{MP}^{FOMC} = 46.5$											
FF Shock	-5.39	-2.42	-3.50	-3.50	-3.93	-4.47	-5.12	-5.28	-5.60	-6.68	-7.49
FF Shock $\times (RA_t > \text{Median})$	-1.99	-0.89	-1.29	-1.29	-1.45	-1.65	-1.89	-1.95	-2.07	-2.47	-2.77

Note: This table shows model robustness for Table 6 in the main paper, but uses different values for the volatility of FOMC date shocks σ_{MP}^{FOMC} . It reports model regressions of the form $r_{j,t}^{FOMC} = b_{j,0} + b_{j,1}\Delta^{FOMC}i_t + b_{j,2}\Delta^{FOMC}i_t(RA_t > \text{Median}) + b_{j,3}(RA_t > \text{Median}) + \varepsilon_{j,t}$. Here, $r_{j,t}^{FOMC}$ is the high-frequency industry or market return around FOMC announcements, and $\Delta^{FOMC}i_t$ is the high-frequency fed funds rate shock. Industries are sorted by their quarterly stock market beta from left to right, as in Table 5. Model data is obtained from a simulation of length 10,000.

E.4. Model Robustness: Varying the Phillips Curve Slope

In this section, we show that our calibration properties in Table 3 and the baseline stock results in Table 4 are insensitive to setting different values for the Phillips curve slope parameter κ . Our baseline results reported in the main paper correspond to $\kappa = 0.0062$. Here, we also report $\kappa = 0$ (i.e. prices are perfectly sticky), and $\kappa = 0.0045$ (price-stickiness parameter $\alpha = 0.9$).

Table A4 Unconditional Quarterly Model Properties

Stocks	Data	Model		
		$\kappa = 0$	$\kappa = 0.0045$	$\kappa = 0.0062$
Equity Premium	7.84	7.11	7.34	7.29
Volatility	16.87	17.31	14.98	14.87
Sharpe Ratio	0.47	0.41	0.49	0.49
AR(1) Coeff. pd	0.92	0.94	0.93	0.93
1-YR Excess Returns on pd	-0.38	-0.29	-0.33	-0.34
1-YR Excess Returns on pd (R^2)	0.23	0.06	0.07	0.07
10-Year Nominal Bonds				
Yield Spread	1.87	1.01	0.99	0.94
Volatility Excess Returns	9.35	4.20	2.86	2.57
1-YR Excess Returns on Yield Spread	2.69	-0.30	-0.20	-0.18
1-YR Excess Returns on Yield Spread (R^2)	0.14	0.01	0.01	0.01
Macroeconomic Dynamics				
Std. Annual Cons. Growth	1.50	1.52	1.54	1.55
Std. Annual Change fed funds Rate	1.35	2.10	2.12	2.13
Trough Output Response to 100 bps fed funds Surprise	-0.70	-0.71	-0.71	-0.71
Lag Trough Output Response (Quarters)	4-6	4	4	4

Table A5 Stock Market onto High-Frequency Monetary Policy Shocks

$\kappa = 0$	Model					
	Overall		Risk Neutral		Risk Premium	
FF Shock	-7.41	-7.34	-1.60	-1.60	-5.81	-5.74
FF Shock x (FF Shock >0)		-0.09		0.00		-0.09
$\kappa = 0.0045$						
FF Shock	-6.41	-6.35	-1.27	-1.26	-5.14	-5.09
FF Shock x (FF Shock >0)		-0.07		-0.02		-0.06
$\kappa = 0.0062$						
FF Shock	-6.37	-6.31	-1.23	-1.22	-5.13	-5.08
FF Shock x (FF Shock >0)		-0.07		-0.02		-0.06

F. Empirical robustness

F.1. Portfolio return regressions

In this Section, we confirm that the cross-sectional results are not specific to industry portfolios, but instead look similar for beta-sorted portfolios, thereby isolating cyclicalities from other industry characteristics such as duration or financial constraints (Ottonello and Winberry (2020)).

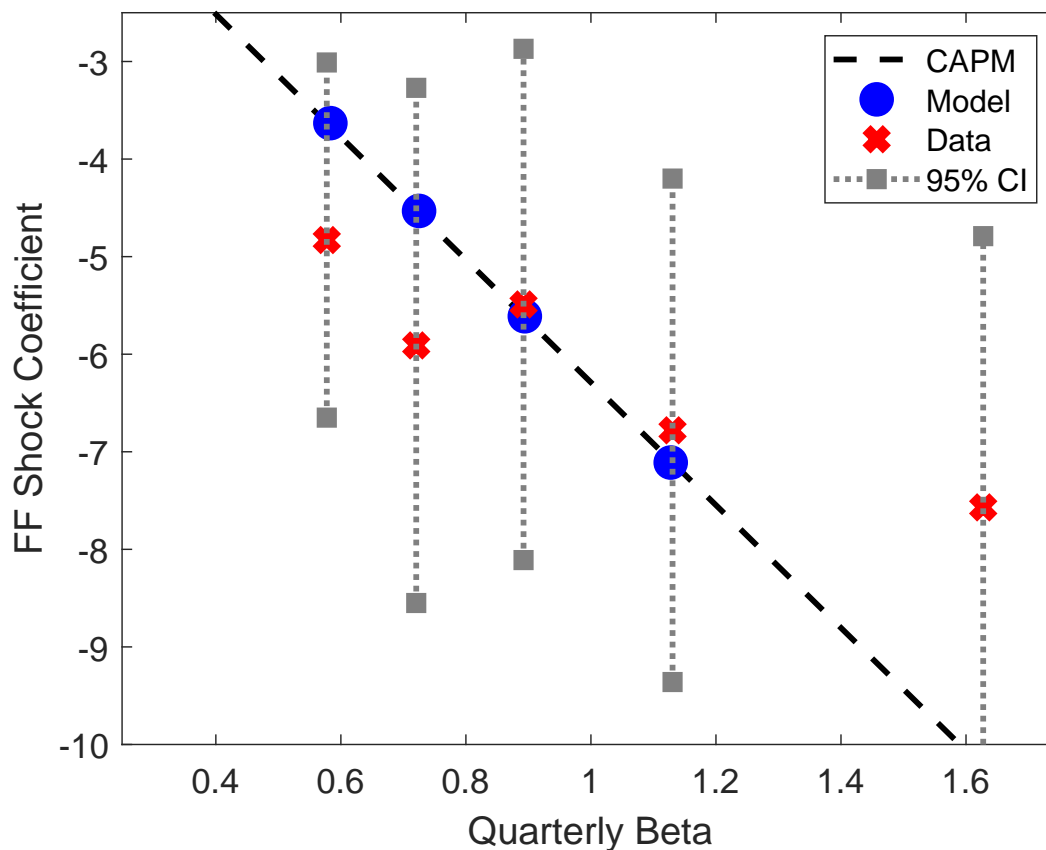
Figure A2 shows the results for beta-sorted portfolios. Beta-sorted portfolios are constructed as follows.

1. Construct a sample of common stocks traded on NYSE, AMEX, and NASDAQ. Obtain the monthly return and market cap for each stock.
2. Estimate market beta for each stock i in month m using a 60-month rolling window. This is the approach for Fama-French portfolios formed on market beta.
 - (a) For stock i in month m , obtain its monthly returns from month $m - 59$ to m .
 - (b) Run the time series regression $retrf_{i,m'} = \beta_m \times mktrf_{i,m'} + \varepsilon_{i,m'}$, using data from the previous step.
 - (c) If there are at least 24 valid observations for the regression in the previous step, then let the estimated $\hat{\beta}_m$ be the beta of stock i in month m . Otherwise, beta is missing.
 - (d) At the end of each quarter q , sort stocks traded on NYSE into 5 portfolios by their beta in quarter q , and use these NYSE beta breakpoints for all the stocks in our sample. This is the approach for Fama-French portfolios formed on market beta.
3. On each FOMC date t (in quarter q), obtain the beta breakpoints at the end of quarter $q - 1$. Then compute the value-weighted return of each quintile portfolio on day t , where the weights are the market cap on day t .

We compute the high-frequency returns for the market, industry portfolios, and beta-sorted portfolios according to Online Appendix A of Nakamura and Steinsson (2018). For security n on day t :

- (a) We find the last trade before 2:05pm on day t and define the associated price as the pre-price $p_t^{pre}(n)$
- (b) We find the first trade within the window [2:35pm on day t ; 12pm on day $t + 1$] and define the associated price as the post-price $p_t^{post}(n)$
- (c) The high-frequency return of security n on day t is defined as $(p_t^{post}(n)/p_t^{pre}(n) - 1) \times 100$
- (d) If either $p_t^{pre}(n)$ or $p_t^{post}(n)$ is missing, then we set the high-frequency return to be missing. If the high-frequency return is 0, then it means we have non-missing $p_t^{pre}(n)$ and $p_t^{post}(n)$, and $p_t^{post}(n) = p_t^{pre}(n)$.

Fig. A2 Beta-Sorted Portfolios



Note: This figure is constructed in the same way as Figure 4 in the main paper, but instead of using industry portfolios it uses five beta-sorted portfolios. 95% confidence intervals for the empirical scaled coefficient $b_{j,1}$ are shown. Stocks are sorted quarterly using betas estimated over a 60-month rolling window and NYSE breakpoints. The results are obtained from a simulation of length 10000.

F.2. Robustness stock response by risk aversion

This Section shows robustness of our empirical finding that stock returns are more sensitive to monetary policy shocks when risk aversion is high. Table A6 repeats the analysis of Table 6 in the main paper without including the $timing_t$ control, and shows that the interaction $FF \times (RA_{t,i} \text{Median})$ remains very similar in magnitude and statistically significant. Further, the coefficients increase monotonically from small and statistically insignificant to large and statistically significant as we go from the lowest beta industries to the highest beta industries.

Tables A7 and A8 show that the interaction is similarly negative and statistically significant when we use a continuous VIX variable rather than a dummy, so our results are not due to splitting the sample in a particular way. Because the VIX variable in Tables A7 and A8 is standardized to have mean zero and a unit standard deviation, the magnitudes are not directly comparable to those in Table 6 in the main paper.

Table A6 Stock Returns onto High-Frequency Monetary Policy Shocks by Risk Aversion - No Timing Control

	Mkt	Utils	NoDur	Hlth	Engry	Shops	Telcm	Manuf	Other	Durbl	HiTec
Data - High-Frequency Regression											
FF Shock	-0.48 (0.47)	-0.99** (0.47)	-0.20 (0.48)	0.16 (0.55)	-0.22 (0.37)	-0.58 (0.50)	-0.41 (0.55)	-0.32 (0.44)	-0.75 (0.64)	0.08 (0.65)	-0.85 (0.71)
FF Shock \times ($RA_t > \text{Median}$)	-4.37*** (1.59)	-1.20 (1.27)	-2.78** (1.20)	-3.20** (1.45)	-3.66** (1.55)	-3.57** (1.47)	-3.70** (1.72)	-4.27*** (1.51)	-5.50** (2.15)	-3.98*** (1.50)	-5.02*** (1.90)
FF Shock \times ($RA_t > \text{Med}$)	-3.25** (1.57)	-0.18 (1.17)	-1.68 (1.14)	-2.26 (1.51)	-2.74* (1.51)	-2.43* (1.46)	-2.37 (1.52)	-3.15** (1.43)	-4.38** (2.15)	-2.74* (1.43)	-3.86** (1.88)
Quarterly Beta											
	1 (0.00)	0.45 (0.08)	0.65 (0.06)	0.65 (0.06)	0.73 (0.09)	0.83 (0.05)	0.95 (0.07)	0.98 (0.05)	1.04 (0.05)	1.24 (0.09)	1.39 (0.07)

Note: This table is identical to Table 6 in the main paper, except that the empirical results do not control for the monetary policy timing variable. This table reports regressions of the form $r_{j,t}^{FOMC} = b_{j,0} + b_{j,1}\Delta^{FOMC}_{i_t} + b_{j,2}\Delta^{FOMC}_{i_t}(RA_t > \text{Median}) + b_{j,3}(RA_t > \text{Median}) + \varepsilon_{j,t}$. Here, $r_{j,t}^{FOMC}$ is the 30 minute industry or market return around FOMC announcements computed from TAQ data. $\Delta^{FOMC}_{i_t}$ is the fed funds rate shock from the current month futures over the same time interval. In the data, we use the VIX to proxy for high risk aversion RA_t while in the model we use the negative surplus consumption ratio. The constant and the dummy coefficient are suppressed in the table. Industries are sorted by their quarterly stock market beta from left to right, as in Table 5. The empirical sample consists of 202 scheduled FOMC announcements from January 1994 until March 2019. Heteroskedasticity adjusted standard errors are reported in parentheses below the empirical estimates. *p<0.1; **p<0.05; ***p<0.01.

Table A7 regresses 30 minute returns on the aggregate stock market and industries onto the 30 minute federal funds rate shock, and the 30 minute federal funds rate shock interacted with the VIX on the day prior to the FOMC announcements, while controlling for $timing_t$. VIX is standardized to have a unit standard deviation. The regressions are analogous to Table 6 in the main paper, but rather than using a VIX dummy we use the continuous VIX variable. Industries are sorted from low to high unconditional quarterly betas. We see that interaction FF Shock \times VIX enters negatively for the market, meaning that the market declines more in response to a high-frequency monetary policy shock in periods when the VIX is high. Going from left to right in the table shows that the interaction coefficient becomes more negative for high-beta industries, such as high-tech, meaning that the state-dependence of the stock return response to a monetary policy shock is stronger for more cyclical industries. Table A7 therefore confirms that the empirical state-dependence of the stock return response across high- and low-risk aversion states is robust to not using a dummy variable. Table A8 shows that results are similar or even larger and more significant when we do not control for timing changes in the policy rate.

Table A7 Empirical State-Dependence with Continuous VIX Variable

	Mkt	Utils	NoDur	Hlth	Enrgy	Shops	Telcm	Manuf	Other	Durbl	HiTec
FF Shock	-6.36*** (1.05)	-4.98*** (0.82)	-5.02*** (0.76)	-4.32*** (0.96)	-5.25*** (1.05)	-6.12*** (1.08)	-6.10*** (0.91)	-5.86*** (0.93)	-7.52*** (1.57)	-6.02*** (1.04)	-7.12*** (1.18)
FF Shock \times VIX	-1.10* (0.57)	0.19 (0.54)	-0.74* (0.44)	-0.96* (0.53)	-1.01* (0.56)	-0.94* (0.51)	-1.39* (0.80)	-1.36** (0.55)	-1.13 (0.76)	-0.98* (0.55)	-1.46** (0.66)
VIX	-0.15*** (0.06)	-0.07 (0.05)	-0.11*** (0.04)	-0.10*** (0.04)	-0.16** (0.06)	-0.15*** (0.05)	-0.14** (0.06)	-0.13** (0.05)	-0.17** (0.08)	-0.16** (0.07)	-0.17*** (0.05)
Const.	-0.06** (0.03)	-0.01 (0.03)	-0.06*** (0.02)	-0.05** (0.02)	-0.07** (0.03)	-0.08*** (0.03)	-0.09*** (0.03)	-0.07** (0.03)	-0.01 (0.06)	-0.07** (0.03)	-0.11*** (0.03)
Nobs	202	202	202	202	202	202	202	202	202	202	202
R^2	0.26	0.16	0.28	0.22	0.22	0.28	0.29	0.30	0.13	0.24	0.27

Note: This table shows robustness for the empirical results in Table 6. It reports regressions of the form $r_{j,t}^{FOMC} = b_{j,0} + b_{j,1}\Delta^{FOMC}i_t + b_{j,2}\Delta^{FOMC}i_t \times VIX_{t-1} + b_{j,3}VIX_{t-1} + b_{j,4}timing_t + \varepsilon_{j,t}$. Here, $r_{j,t}^{FOMC}$ is the 30 minute industry or market return around FOMC announcements from TAQ and $\Delta^{FOMC}i_t$ is the fed funds rate shock from current month futures over the same time interval. The coefficient on the monetary policy timing variable $timing_t$ is suppressed. This table uses the VIX directly, whereas in the main paper we use a dummy indicating whether the VIX is above or below its full-sample median. VIX is standardized to have a unit standard deviation. The empirical sample consists of 202 scheduled FOMC announcements from February 1994 until March 2019. Heteroskedasticity adjusted standard errors are reported in parentheses below the empirical estimates. *p<0.1; **p<0.05; ***p<0.01.

Table A8 Empirical State-Dependence with Continuous VIX Variable - No Timing Control

	Mkt	Utils	NoDur	Hlth	Enrgy	Shops	Telcm	Manuf	Other	Durbl	HiTec
FF Shock	-2.68*** (0.78)	-1.67*** (0.64)	-1.55*** (0.56)	-1.37** (0.69)	-2.10*** (0.76)	-2.38*** (0.72)	-2.07*** (0.71)	-2.36*** (0.70)	-3.64*** (1.16)	-1.94*** (0.73)	-3.34*** (0.91)
FF Shock \times VIX	-1.68*** (0.61)	-0.33 (0.60)	-1.28*** (0.49)	-1.42*** (0.51)	-1.51** (0.61)	-1.52*** (0.53)	-2.02** (0.91)	-1.91*** (0.60)	-1.74** (0.79)	-1.63*** (0.59)	-2.05*** (0.67)
VIX	-0.12** (0.06)	-0.05 (0.05)	-0.09** (0.04)	-0.08** (0.04)	-0.14** (0.06)	-0.13** (0.05)	-0.11* (0.06)	-0.10** (0.05)	-0.14* (0.09)	-0.13* (0.07)	-0.14*** (0.05)
Const.	-0.05 (0.03)	0.00 (0.03)	-0.05** (0.02)	-0.04 (0.02)	-0.06** (0.03)	-0.07** (0.03)	-0.07** (0.03)	-0.05* (0.03)	0.00 (0.06)	-0.06* (0.03)	-0.09** (0.03)
N	202	202	202	202	202	202	202	202	202	202	202
R^2	0.17	0.05	0.13	0.12	0.15	0.16	0.16	0.19	0.09	0.13	0.19

Note: This table shows robustness for the empirical results in Table 6. It reports regressions of the form $r_{j,t}^{FOMC} = b_{j,0} + b_{j,1}\Delta^{FOMC}i_t + b_{j,2}\Delta^{FOMC}i_t \times VIX_{t-1} + b_{j,3}VIX_{t-1} + \varepsilon_{j,t}$. Here, $r_{j,t}^{FOMC}$ is the 30 minute industry or market return around FOMC announcements from TAQ and $\Delta^{FOMC}i_t$ is the fed funds rate shock over the same time interval. This table uses the VIX directly, whereas in the main paper we use a dummy indicating whether the VIX is above or below its full-sample median. VIX is standardized to have a unit standard deviation. The empirical sample consists of 202 scheduled FOMC announcements from February 1994 until March 2019. Heteroskedasticity adjusted standard errors are reported in parentheses below the empirical estimates. *p<0.1; **p<0.05; ***p<0.01.

Tables A9, A10, and A11 analyze the ability of the dividend-price ratio to explain variation in the stock return response to monetary policy shocks. While the dividend-price ratio is the most direct measure of risk aversion within our model, it also comes with issues for the analysis that we run, leading us to prefer the VIX for our main analysis. For this robustness exercise, we use the log dividend price ratio minus a ten year moving average to account for the shift towards persistently higher stock prices after the late 1990s, and split the sample into periods with above- and below-median dividend price ratios. While the interaction between the fed funds shock and $(dp_t)_i$ Median enters negatively in Table A9, as expected, this interaction is not statistically significant.

However, Table A10 shows that the interaction coefficients become larger in magnitude and significant for some industry portfolios when we do not control for the $timing_t$ variable that captures shifts in the timing of policy rate changes. One possibility why it might be better to not control for $timing_t$ in this analysis could be if $timing_t$ is heteroskedastic in such a way that it is more volatile and correlated with the fed funds shock when dp_t is high. Such heteroskedasticity is not implausible, given that the Fed has shifted towards forward guidance as a monetary policy tool after stock market crashes, such as the 2001 dotcom bust and 2008-2009.

Because simple de-trending may not appropriately adjust the dividend-price ratio, Table A11 also analyzes the stock market response to monetary policy shocks by dividend-price ratio starting in 2002, which is arguably after the persistent shift in stock prices. This table shows that once we exclude the pre-2002 period, the interaction FF Shock x $(dp_t)_i$ Med becomes negative and statistically significant, though still estimated with substantial noise.

Overall, it appears that our conclusions are robust to using the dividend-price ratios, at least once the shift in the overall level of stock prices and potentially changing monetary policy instruments are accounted for. However, we still prefer the VIX as our baseline measure, especially within the broader interpretation of our model as capturing countercyclical risk aversion.

Table A9 Stock Returns onto High-Frequency Monetary Policy Shocks by Dividend-Price Ratio

	Mkt	Utils	NoDur	Hlth	Enrgy	Shops	Telcm	Manuf	Other	Durbl	HiTec
Data - High-Frequency Regression											
FF Shock	-5.62*** (1.30)	-4.13*** (0.74)	-4.19*** (0.92)	-3.67*** (1.13)	-3.07*** (0.98)	-5.28*** (1.19)	-5.56*** (1.22)	-5.05*** (1.12)	-7.21*** (2.19)	-4.58*** (1.10)	-6.56*** (1.51)
FF Shock \times ($dp_t > \text{Med}$)	-1.21 (1.94)	-0.39 (1.53)	-0.97 (1.41)	-1.27 (1.76)	-3.21 (1.97)	-0.95 (1.79)	-1.09 (1.92)	-1.77 (1.78)	-0.97 (2.59)	-2.08 (1.74)	-0.82 (2.21)
($dp_t > \text{Med}$)	-0.09 (0.06)	-0.01 (0.05)	0.01 (0.05)	-0.03 (0.05)	-0.04 (0.06)	-0.05 (0.06)	-0.01 (0.06)	-0.05 (0.05)	-0.29*** (0.11)	-0.08 (0.06)	-0.01 (0.07)
Const.	-0.01 (0.04)	-0.00 (0.03)	-0.06** (0.03)	-0.03 (0.03)	-0.05* (0.03)	-0.05 (0.04)	-0.08** (0.03)	-0.04 (0.03)	0.14 (0.09)	-0.03 (0.03)	-0.09* (0.05)
N	202	202	202	202	202	202	202	202	202	202	202
R^2	0.19	0.13	0.20	0.16	0.14	0.18	0.20	0.22	0.12	0.16	0.18

Note: This table reports regressions of the form $r_{j,t}^{FOMC} = b_{j,0} + b_{j,1}\Delta^{FOMC}i_t + b_{j,2}\Delta^{FOMC}i_t(RA_t > \text{Median}) + b_{j,3}(RA_t > \text{Median}) + \varepsilon_{j,t}$. Here, $r_{j,t}^{FOMC}$ is the 30 minute industry or market return around FOMC announcements computed from TAQ data. $\Delta^{FOMC}i_t$ is the fed funds surprise implied by the current month fed funds futures over the same time interval. In the data, we use the dividend price ratio minus a 10-year moving average to proxy for high risk aversion RA_t while in the model we use the negative surplus consumption ratio. The constant and the dummy coefficient are suppressed in the table. Industries are sorted by their quarterly stock market beta from left to right, as in Table 5. The empirical sample consists of 202 scheduled FOMC announcements from January 1994 until March 2019. Heteroskedasticity adjusted standard errors are reported in parentheses below the empirical estimates. *p<0.1; **p<0.05; ***p<0.01.

Table A10 Stock Returns onto High-Frequency Monetary Policy Shocks by Dividend-Price Ratio - No Timing Control

	Mkt	Utils	NoDur	Hlth	Enrgy	Shops	Telcm	Manuf	Other	Durbl	HiTec
Data - High-Frequency Regression											
FF Shock	-1.86** (0.80)	-0.95** (0.40)	-0.76 (0.55)	-0.61 (0.64)	-0.45 (0.38)	-1.59** (0.66)	-1.32** (0.61)	-1.40** (0.62)	-2.92* (1.55)	-0.64 (0.65)	-2.72** (1.05)
FF Shock \times ($dp_t > \text{Med}$)	-2.66 (2.07)	-1.62 (1.61)	-2.30 (1.53)	-2.45 (1.82)	-4.22** (1.99)	-2.37 (1.88)	-2.73 (2.21)	-3.18 (1.96)	-2.62 (2.70)	-3.60* (1.87)	-2.30 (2.38)
($dp_t > \text{Med}$)	-0.06 (0.06)	0.02 (0.06)	0.04 (0.05)	-0.00 (0.05)	-0.02 (0.06)	-0.02 (0.06)	0.03 (0.06)	-0.02 (0.06)	-0.26** (0.11)	-0.05 (0.07)	0.03 (0.07)
Const.	-0.01 (0.04)	-0.00 (0.03)	-0.07** (0.03)	-0.03 (0.03)	-0.05* (0.03)	-0.05 (0.04)	-0.08** (0.04)	-0.04 (0.03)	0.14 (0.09)	-0.03 (0.04)	-0.10* (0.05)
N	202	202	202	202	202	202	202	202	202	202	202
R^2	0.11	0.05	0.08	0.07	0.10	0.09	0.09	0.13	0.08	0.08	0.12

Note: This table is analogous to Table A9 but it does not control for the monetary policy timing variable.

Table A11 Stock Returns onto High-Frequency Monetary Policy Shocks by Dividend-Price Ratio 2002-2019 Sample

	Mkt	Utils	NoDur	Hlth	Enrgy	Shops	Telcm	Manuf	Other	Durbl	HiTec
Data - High-Frequency Regression											
FF Shock	7.57 (5.92)	-3.78 (4.69)	4.51 (4.95)	6.73 (4.53)	-5.72 (6.13)	12.77* (6.55)	7.97 (5.71)	5.09 (5.64)	7.80 (6.49)	12.07* (7.22)	11.18 (7.06)
FF Shock \times ($dp_t > \text{Med}$)	-14.33** (6.10)	-0.95 (4.81)	-9.42* (5.05)	-11.72** (4.72)	-1.12 (6.23)	-18.87*** (6.69)	-14.74** (5.91)	-12.05** (5.81)	-16.09** (6.72)	-18.98** (7.31)	-17.83** (7.23)
($dp_t > \text{Med}$)	-0.12* (0.06)	-0.04 (0.07)	-0.01 (0.06)	-0.08 (0.06)	-0.07 (0.08)	-0.11* (0.06)	-0.07 (0.07)	-0.10 (0.06)	-0.21*** (0.08)	-0.15** (0.08)	-0.13* (0.07)
Const.	(0.05)	(0.06)	(0.04)	(0.04)	(0.06)	(0.04)	(0.05)	(0.05)	(0.05)	(0.05)	(0.05)
N	138	138	138	138	138	138	138	138	138	138	138
R^2	0.20	0.10	0.16	0.17	0.14	0.18	0.18	0.21	0.20	0.16	0.18

Note: This table is analogous to Table A9 but it uses a sample starting in January 2002.

APPENDIX REFERENCES

- Ball, Laurence, and David Romer, 1990, Real rigidities and the non-neutrality of money, *Review of Economic Studies*, 57, 183-203.
- Calvo, Guillermo A, 1983, Staggered prices in a utility-maximizing framework, *Journal of Monetary Economics*, 12, 383-398.
- Campbell, John Y, and John Ammer, 1993, What moves the stock and bond markets? A variance decomposition for long-term asset returns, *Journal of Finance* 48, 3-37.
- Campbell, John Y, and John H Cochrane, 1999, By force of habit, *Journal of Political Economy* 107, 205-251.
- Campbell, John Y, and Sydney Ludvigson, 2001, Elasticities of substitution in real business cycle models with home production, *Journal of Money, Credit and Banking* 33, 847-875.
- Campbell, John Y, Carolin Pflueger, and Luis M Viceira, 2020, Macroeconomic drivers of bond and equity risks, *Journal of Political Economy* 128, 3148-3185.
- Chodorow-Reich, Gabriel, and Loukas Karabarbounis, 2016, The cyclical cost of the opportunity cost of employment, *Journal of Political Economy* 124, 1563-1618.
- Christiano, Lawrence H., Martin Eichenbaum, and Charles L. Evans, 2005, Nominal rigidities and the dynamic effects of a shock to monetary policy, *Journal of Political Economy*, 113, 1-45.
- Cogley, Timothy, and Argia M. Sbordone, 2008, The time-varying volatility of macroeconomic fluctuations, *American Economic Review* 98, 2101-2126.
- Greenwood, Jeremy, Zvi Hercowitz, and Gregory W Huffman, 1988, Investment, capacity utilization, and the real business cycle, *American Economic Review* pp. 402-417.
- Hanson, Samuel G, and Jeremy C Stein, 2015, Monetary policy and long-term real rates, *Journal of Financial Economics* 115, 429-448.
- Kehoe, Patrick J, Pierlauro Lopez, Virgiliu Midrigan, and Elena Pastorino, 2019, Asset prices and unemployment fluctuations, Discussion paper, National Bureau of Economic Research.
- Lettau, Martin, and Harald Uhlig, 2000, Can habit formation be reconciled with business cycle facts?, *Review of Economic Dynamics* 3, 79-99.
- Lopez, Pierlauro, J. David, 2014, Macro-finance separation by force of habit, unpublished paper, Federal Reserve Board and Banque de France.
- Lucas, Robert E. Jr., 1988, On the mechanics of economic development, *Journal of Monetary Economics*, 22, 3-42.
- Nakamura, Emi, and Jon Steinsson, 2018, High-frequency identification of monetary nonneutrality: the information effect, *Quarterly Journal of Economics* 133, 1283-1330.
- Rudebusch, Glenn D, and Eric T Swanson, 2008, Examining the bond premium puzzle with a DSGE model, *Journal of Monetary Economics* 55, 111-126.
- Smets, Frank, and Rafael Wouters, 2007, Shocks and frictions in us business cycles: A Bayesian DSGE approach, *American Economic Review* pp. 586-606.
- Uhlig, Harald, 2007, Explaining asset prices with external habits and wage rigidities in a DSGE model, *American Economic Review*, 97, 239-243.
- Wachter, Jessica A., 2005, Solving models with external habit, *Finance Research Letters* 2, 210-226.
- Walsh, Carl E, 2017, *Monetary Theory and Policy* (MIT press).
- Woodford, Michael, 2003, *Interest and Prices* (Princeton University Press)